Subgrid and direct numerical simulation modeling of turbulence in galaxies and clusters

Evan Scannapieco
ASU School of Earth and Space Exploration

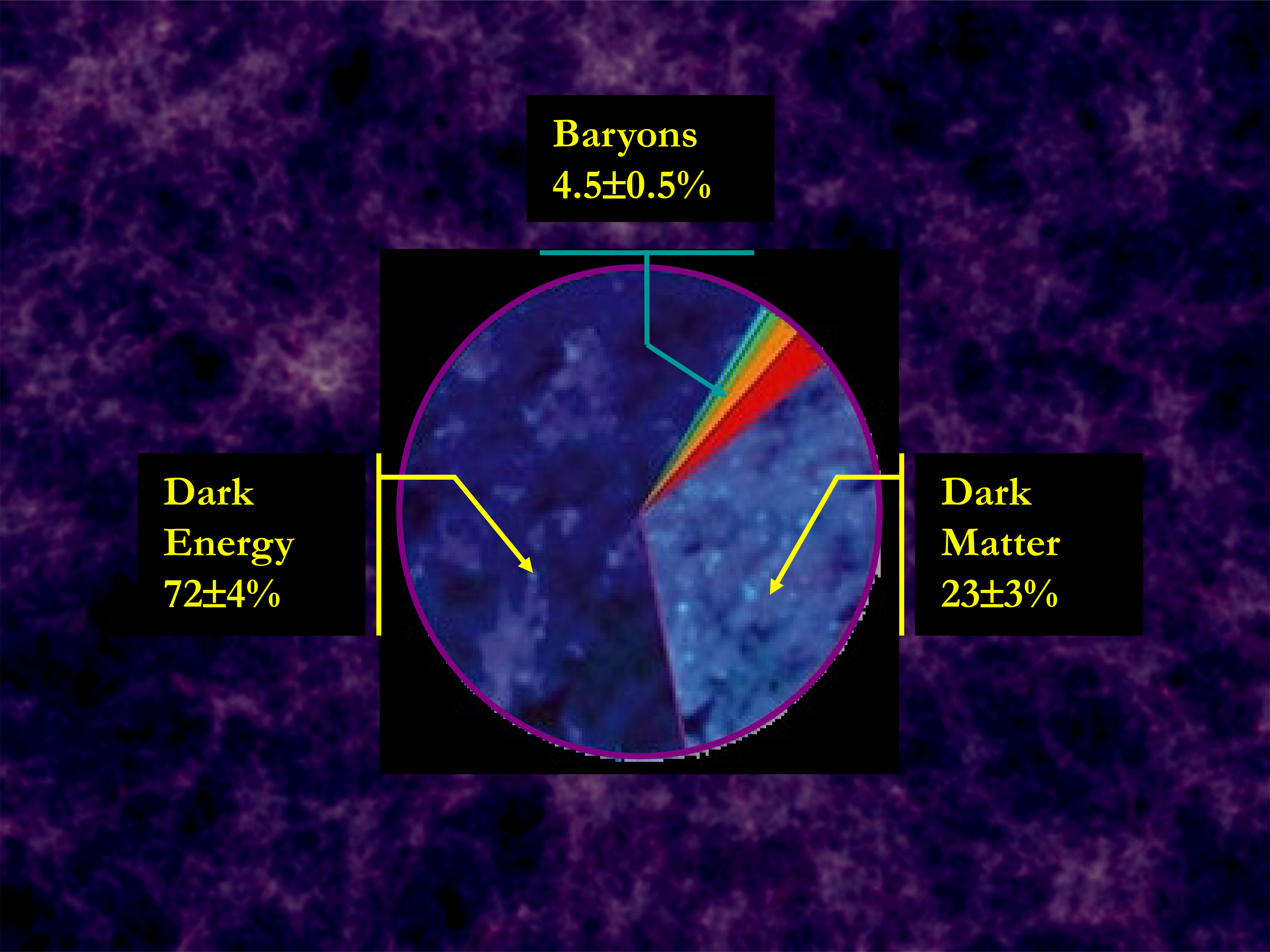
Baryons
4.5±0.5%
Dark
Energy
72±4%
Dark
Matter
23±3%

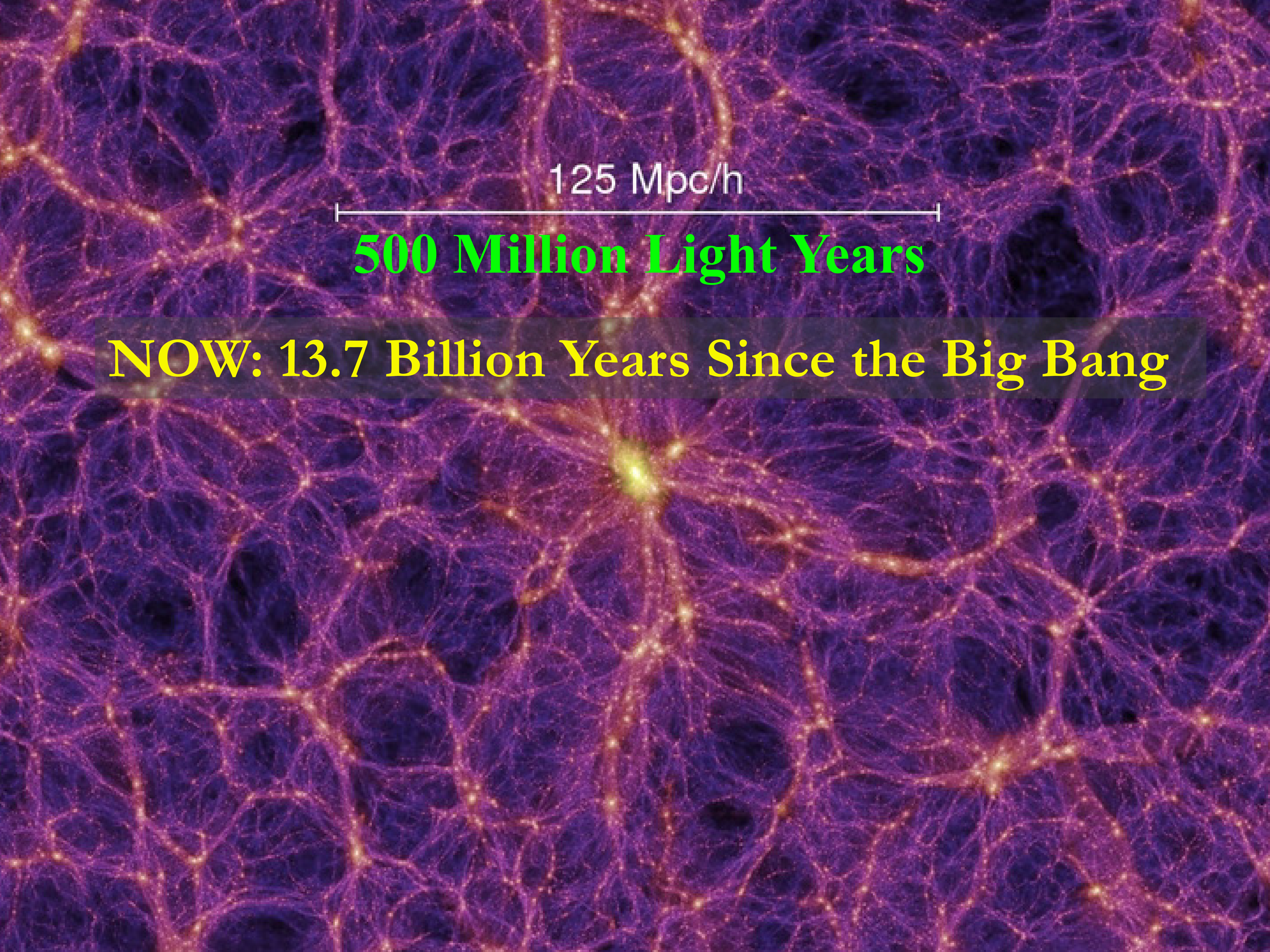
125 Mpc/h
500 Million Light Years
NOW: 13.7 Billion Years Since the Big Bang

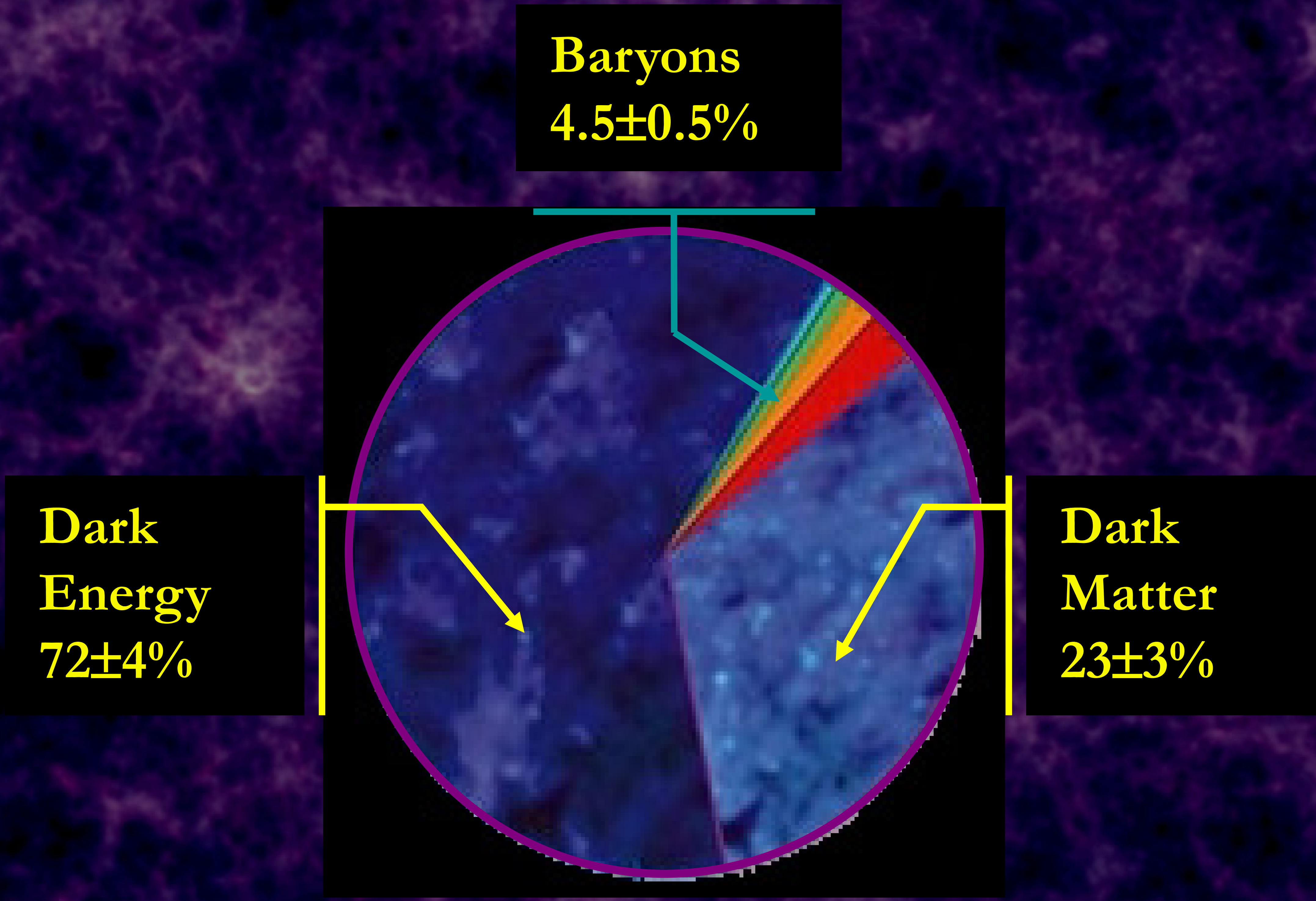
Baryons
4.5±0.5%
Dark
Energy
72±4%
Dark
Matter
23±3%

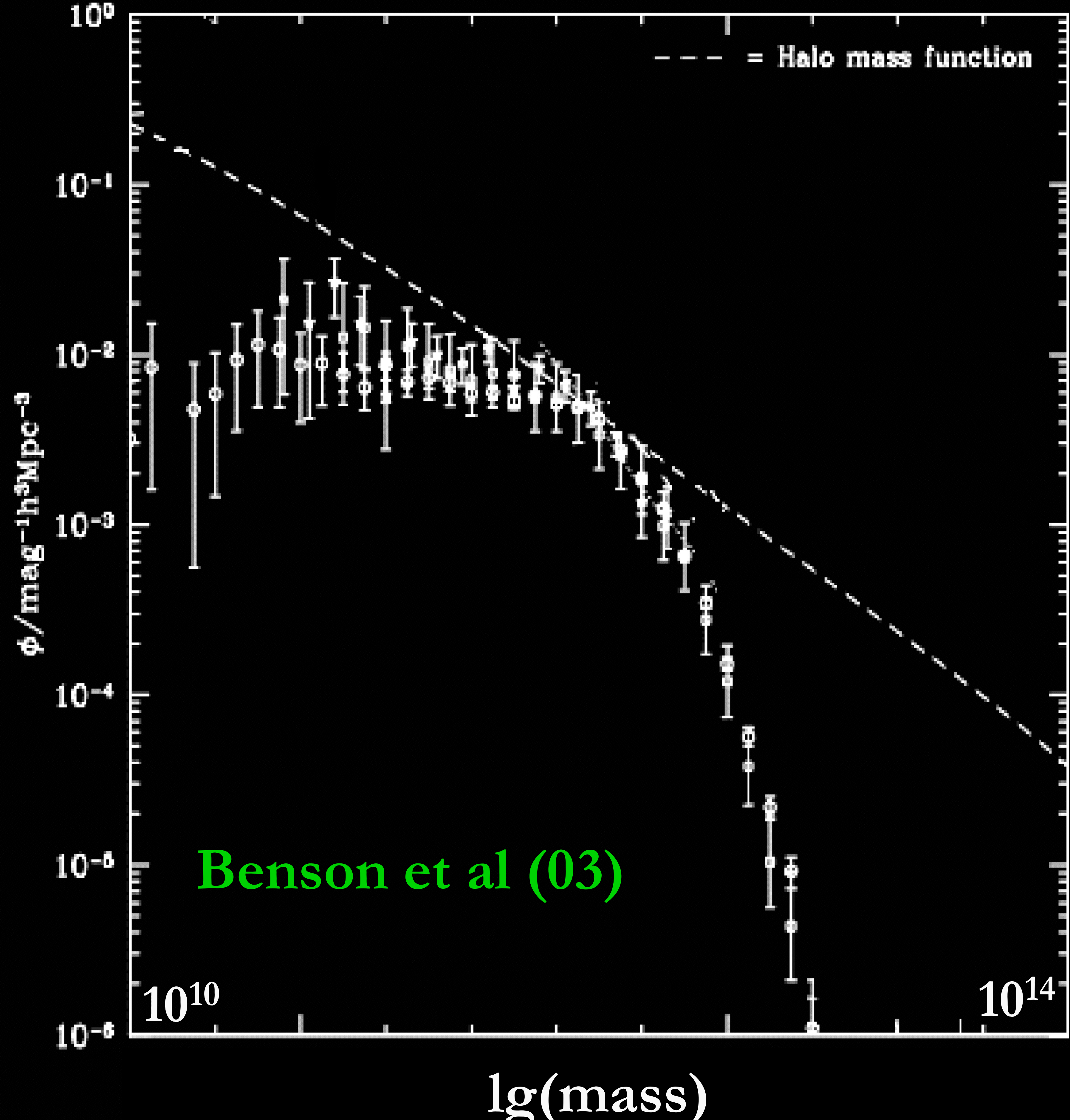

10⁰
10⁻¹
10⁻²
10⁻³
10⁻⁴
10⁻⁵
10⁻⁶
φ/mag⁻¹h³Mpc⁻³
- - - = Halo mass function
Benson et al (03)
10¹⁰
10¹⁴
lg(mass)

I. Low Mass Feedback

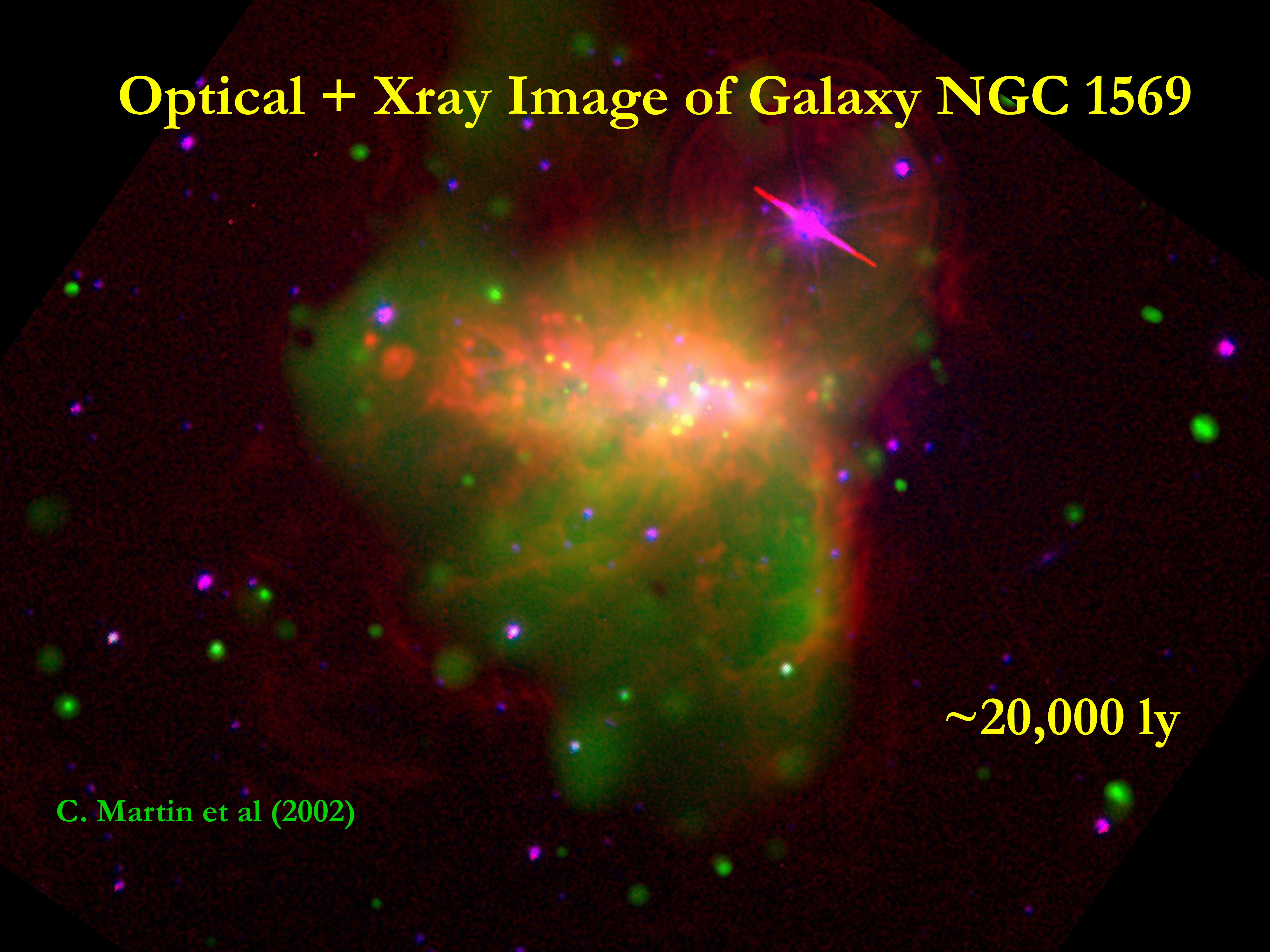
Optical + Xray Image of Galaxy NGC 1569
~20,000 ly
C. Martin et al (2002)

Supernovae & Cooling

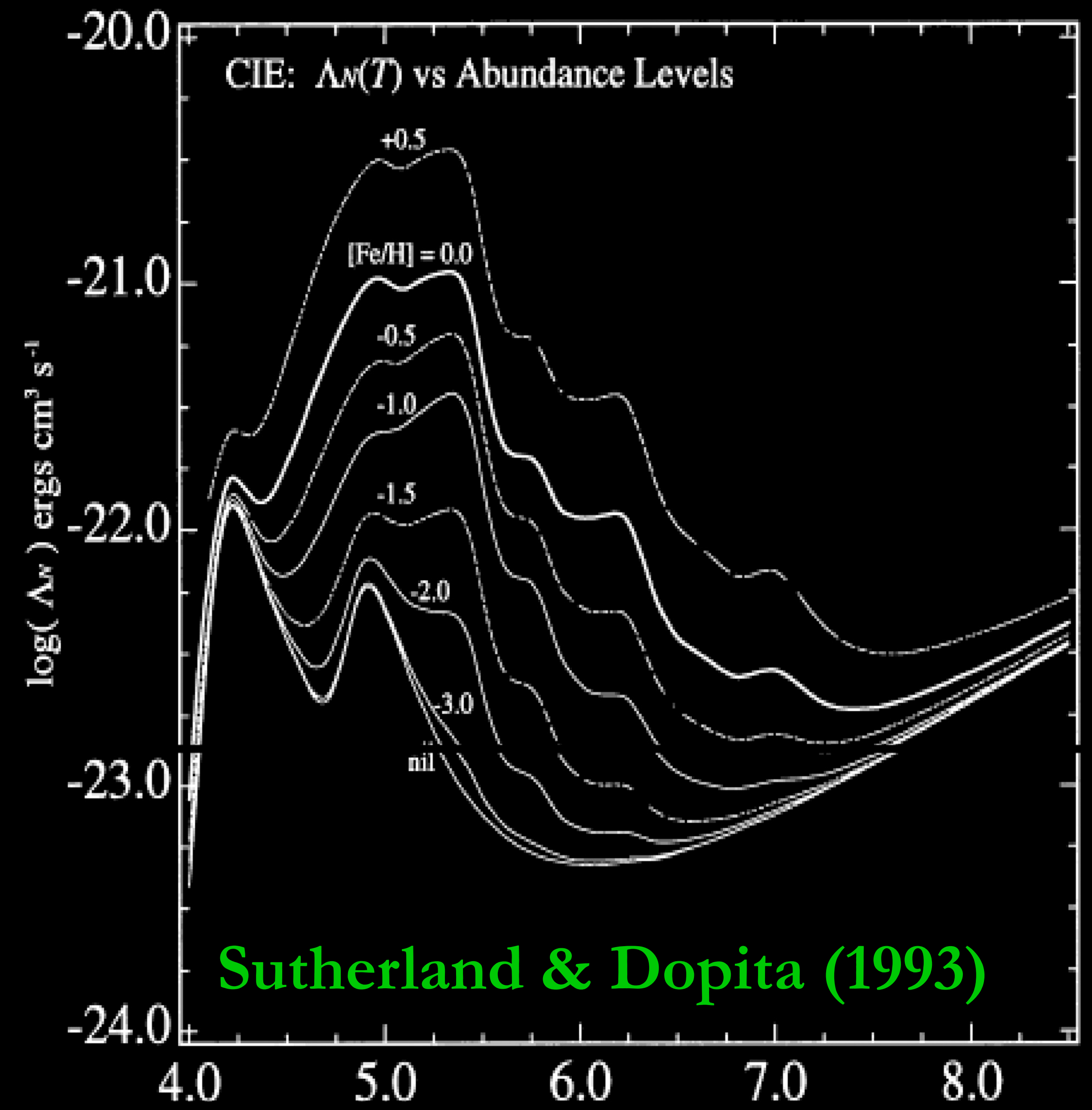

Log T

~10 ly

Cooling times ~ 3000 years

MacLow & Ferrara (1999)

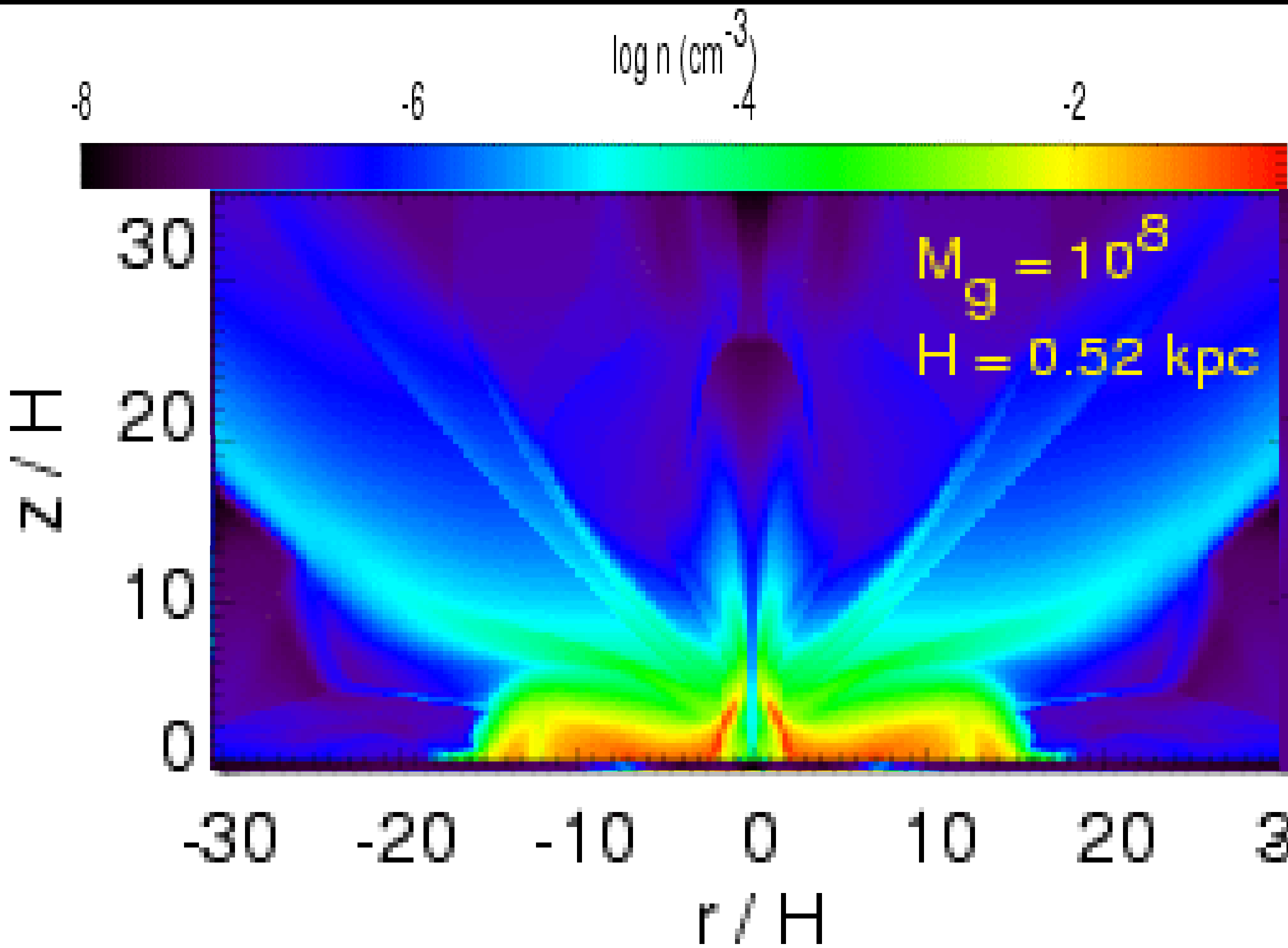

Strickland & Stevens (2000)

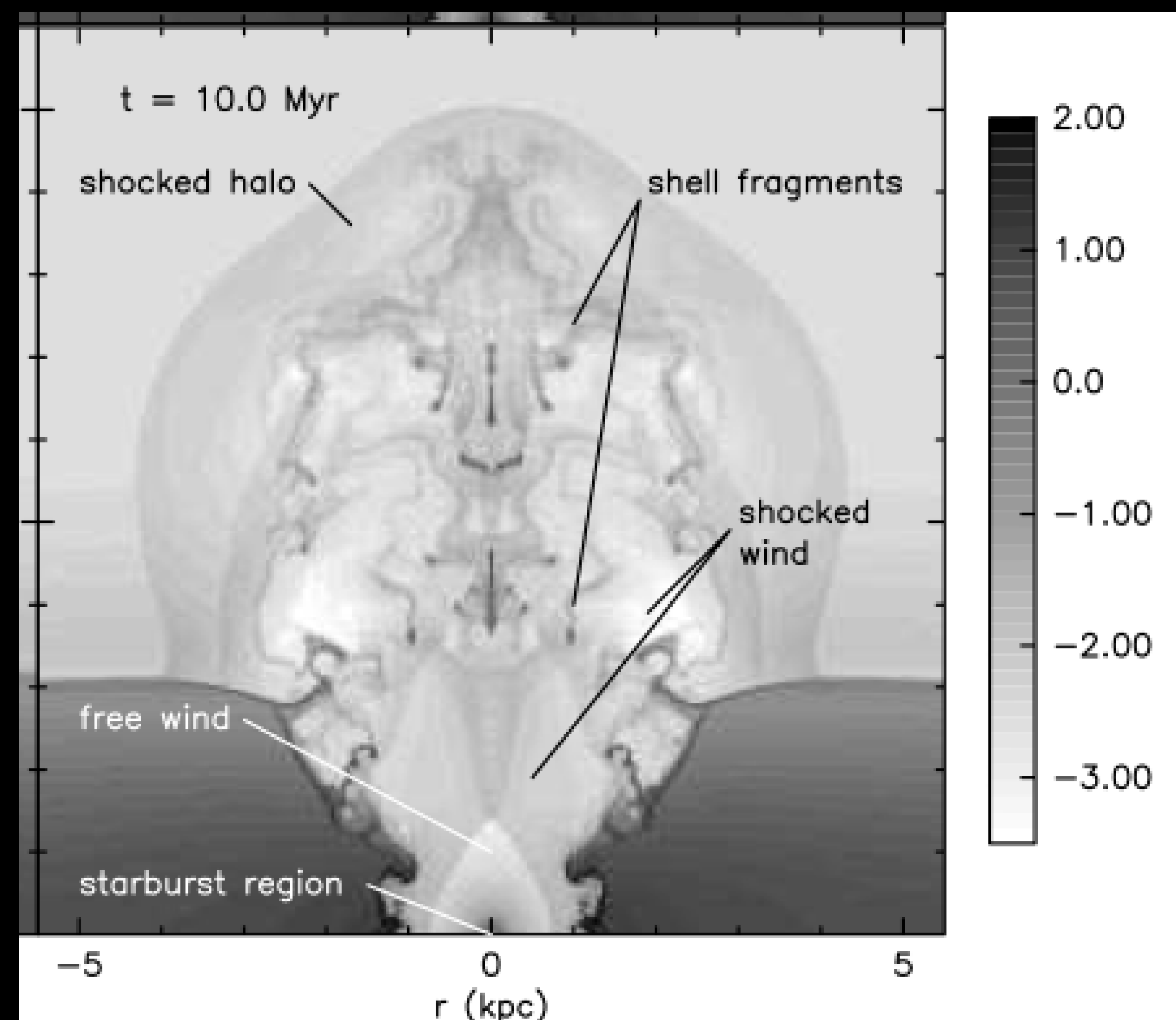

Turbulent Dissipation Scale

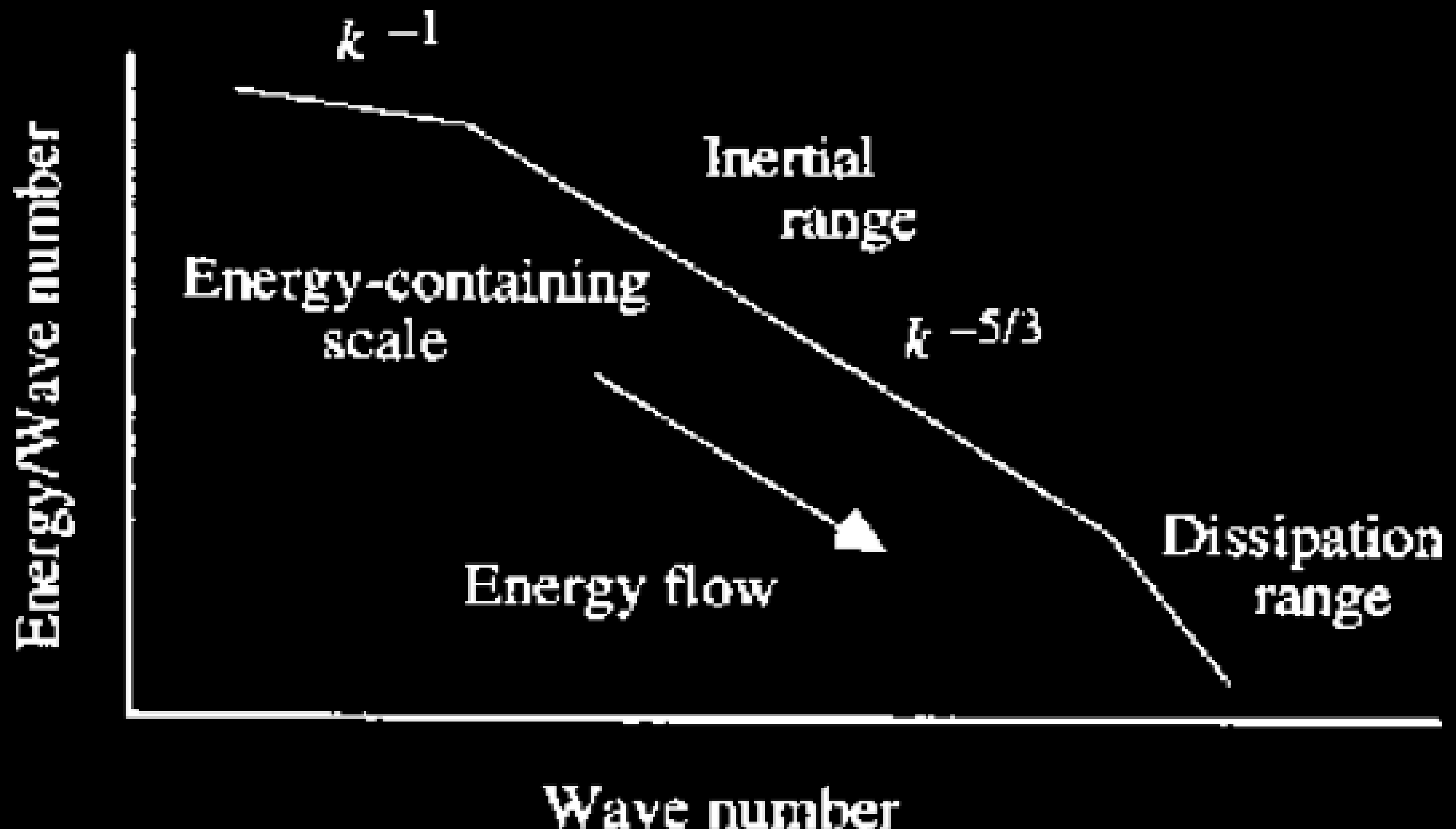

Ionized Medium

Spitzer :

$L \approx 10^{-2}$ ly

Neutral Medium

Ambipolar Diffusion :

$L \approx 10^{-3}$ ly

Supersonic Turbulence

$\vec{V}$

ρ

T

$P(\rho,T)$

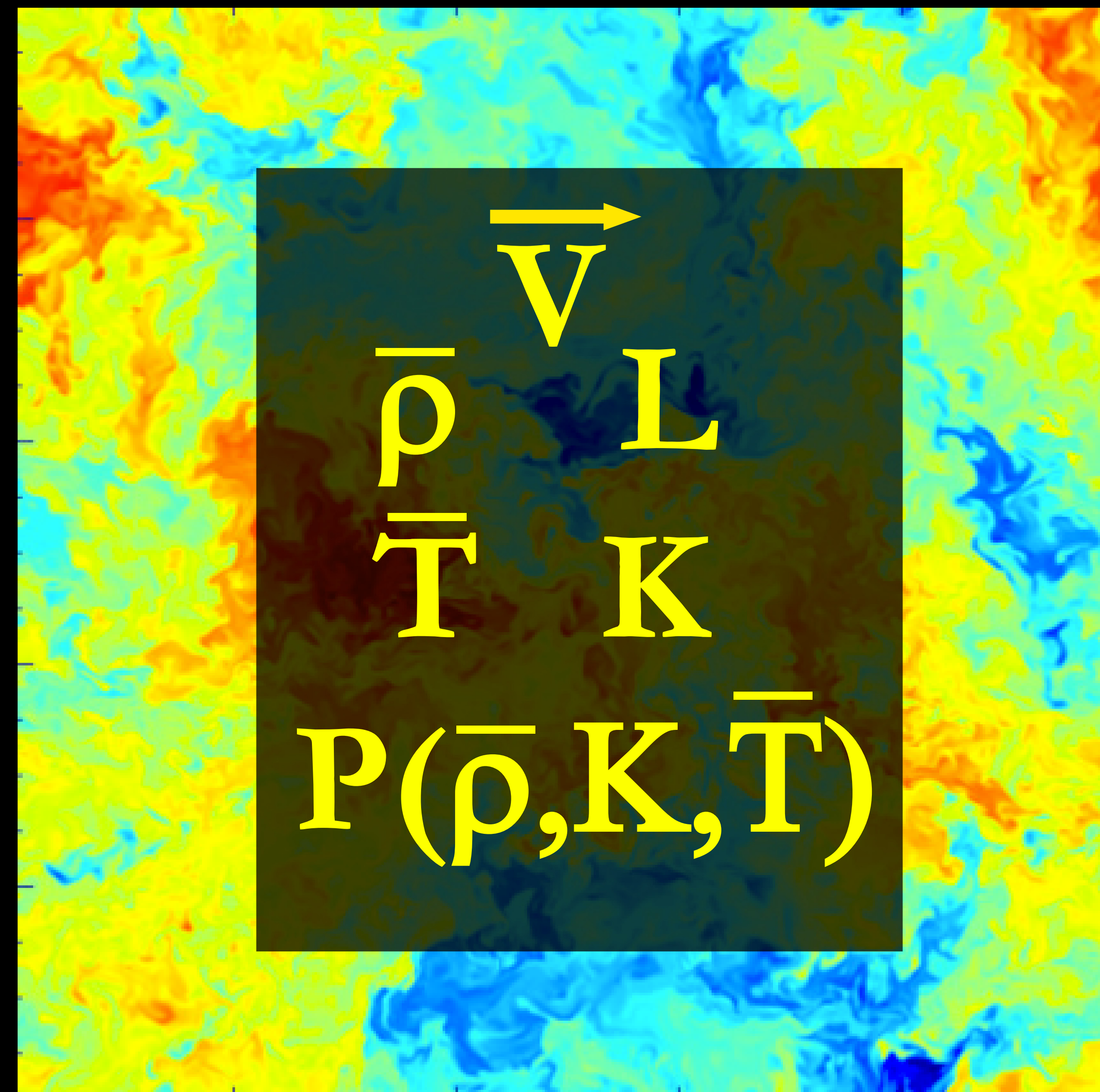

Cooling Time/
Homogeneous composition

ES & M. Bruggen (2010)

Turbulent Decay of Energy
Turbulent Mixing

Cascade Picture for Energy Dissipation and Turbulent Mixing

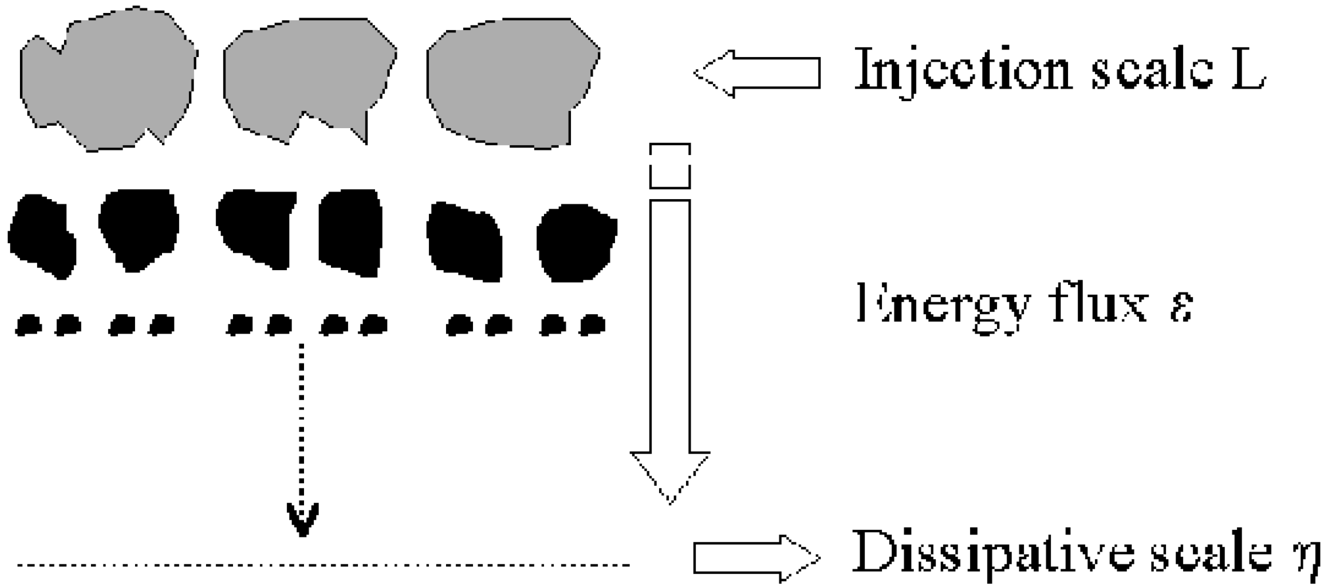

Velocity

Scalar

In incompressible turbulence:

Kolmogorov's similarity hypothesis:

$\delta\upsilon(l) \sim \bar{\varepsilon}^{1/3} l^{1/3}$ and $E(k) \sim \bar{\varepsilon}^{2/3} k^{-5/3}$

Energy decay timescale $\tau_v \sim L / V$

Classic mixing theory (Obukohov--Corrsin) :

$$\delta C(l)^2 \sim \bar{\varepsilon}_C \frac{l}{\delta\upsilon(l)}$$

Mixing timescale τ_c also $\sim L/V$, about $\tau_v/2$.

In supersonic turbulence:

Spectrum steepens with the Mach number (e.g, Kritsuk et al. 2007)

Energy decays at a timescale $\tau_v \sim L / V$ for all Mach numbers (Stone et al. 1998, Mac Low 1999, Padoan & Norlund 1999, Lemaster and Stone 2009)

Does the scalar structure function and spectrum flatten with Mach number?

What is the mixing timescale as a function of the Mach number?

Simulations of Mixing in Supersonic Turbulence

We use the FLASH code with modified "Stir unit" for flow and scalar driving. Periodic simulation box, 512^3 computation cells

Turbulent flows:

- -Driven and maintained by a solenoidal external force at large scales $1 \leq k \leq 3$
- -Amplitude of the force adjusted to obtain 6 Mach numbers from 0.9 to 6
- -Isothermal equation of state.

Passive scalars:

- -Same driving scheme used representing new sources of pollutants at large scales.
- -Three independent scalars evolved in each flow to achieve accurate statistical measurements.

Pan & ES (2010)

x-velocity | concentration

M = 0.9

M = 6.1

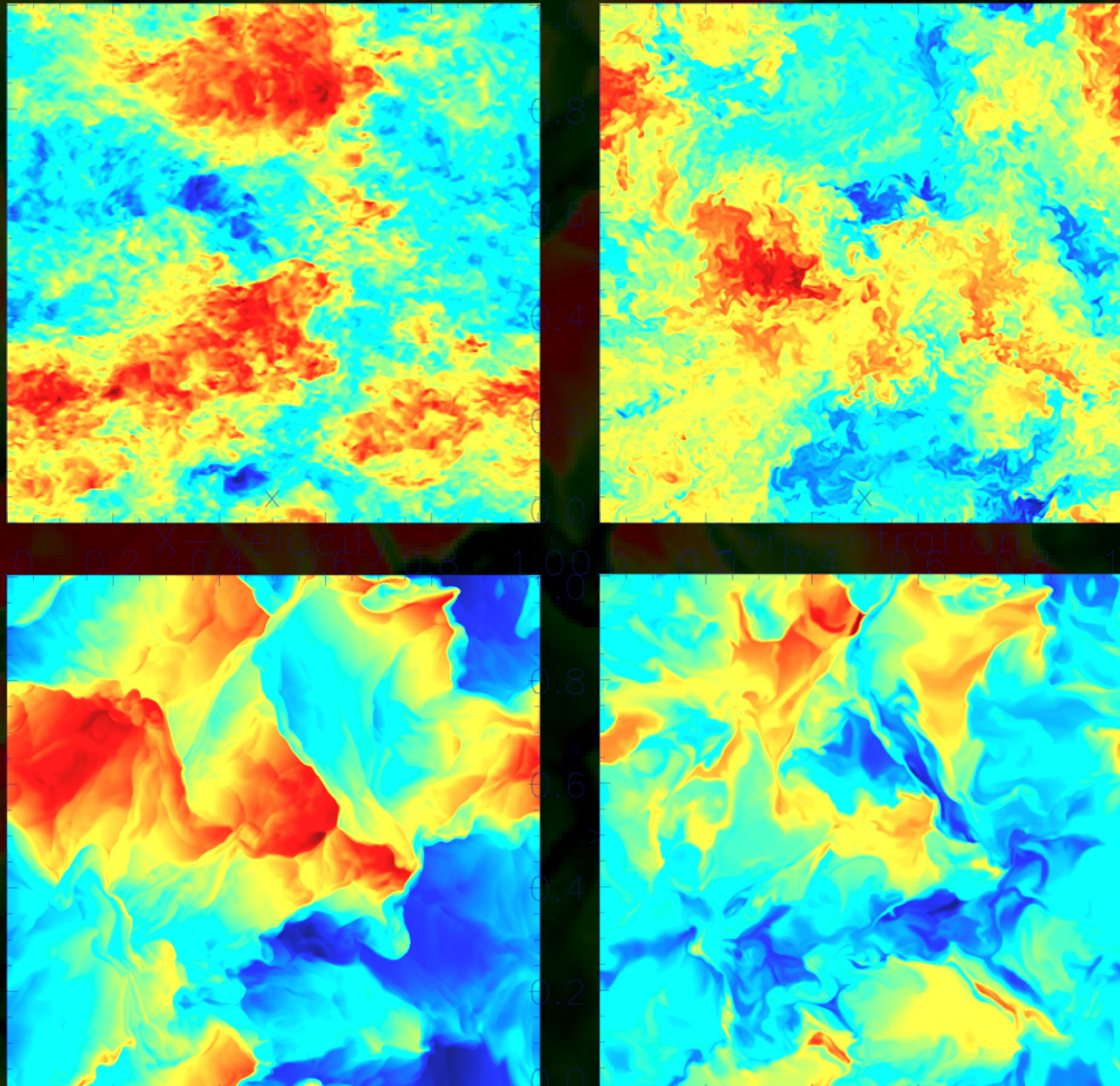

Pan & ES (2010)

Properties of Supersonic Flows as a Function of M

M	$\langle\tilde{\rho}(\nabla\cdot v)^2\rangle/\langle\tilde{\rho}(\nabla\times v)^2\rangle$	$\langle(\nabla\cdot v)^2\rangle/\langle(\nabla\times v)^2\rangle$	f_{comp}	$f_{comp}(k/2\pi \geqslant 4)$
0.9	0.06	0.06	0.05	0.07
1.4	0.19	0.20	0.10	0.16
2.1	0.41	0.49	0.15	0.25
3.0	0.52	0.75	0.17	0.30
4.6	0.55	0.88	0.18	0.33
6.1	0.54	0.86	0.19	0.32

1. The divergence to vorticity ratio increases with M for M < 3, and appears to saturate at M>3. This indicates that compressible modes contributed more to energy dissipation with increasing M for M<3.

2. The fraction of kinetic energy contained in compressible modes first increases with M and then saturates at 1/3 for M>3, corresponding to energy equipartition between the two modes.

Hydrodynamic and Concentration Equations

Hydro:

$$\partial_t \rho + \partial_i(\rho \upsilon_i) = 0$$

$$\partial_t \upsilon_i + \upsilon_j \partial_j \upsilon_i = -\frac{\partial_i p}{\rho} + \frac{\partial_j \sigma_{ij}}{\rho} + f_i$$

where the viscous stress tensor $\sigma_{ij} = \rho \nu (\partial_i \upsilon_j + \partial_j \upsilon_i - \frac{2}{3}\delta_{ij}\partial_k \upsilon_k)$

EOS:

$$p = \rho C_s^2$$

Concentration:

$$\partial_t C + \upsilon_i \partial_i C = \frac{1}{\rho}\partial_i(\rho \kappa \partial_i C) + S$$

C is the *ratio* of the tracer density to the flow density

Concentration variance:

$$\partial_t \langle \tilde{\rho} C^2 \rangle + \partial_i \langle \tilde{\rho} C^2 \upsilon_i \rangle = -2\langle \tilde{\rho}\kappa (\partial_i C)^2 \rangle + 2\langle \tilde{\rho} S C \rangle$$

Kinetic energy:

$$\partial_t \langle \frac{1}{2}\tilde{\rho}\upsilon^2 \rangle + \partial_i \langle \frac{1}{2}\tilde{\rho}\upsilon^2 \upsilon_i \rangle = \frac{\langle p \partial_i \upsilon_i \rangle}{\bar{\rho}} - \frac{1}{2}\langle \tilde{\rho}\nu (\partial_i \upsilon_j + \partial_j \upsilon_i - \frac{2}{3}\delta_{ij}\partial_k \upsilon_k)^2 \rangle + \langle \tilde{\rho} f_i \upsilon_i \rangle$$

Mixing and Energy Dissipation Timescales

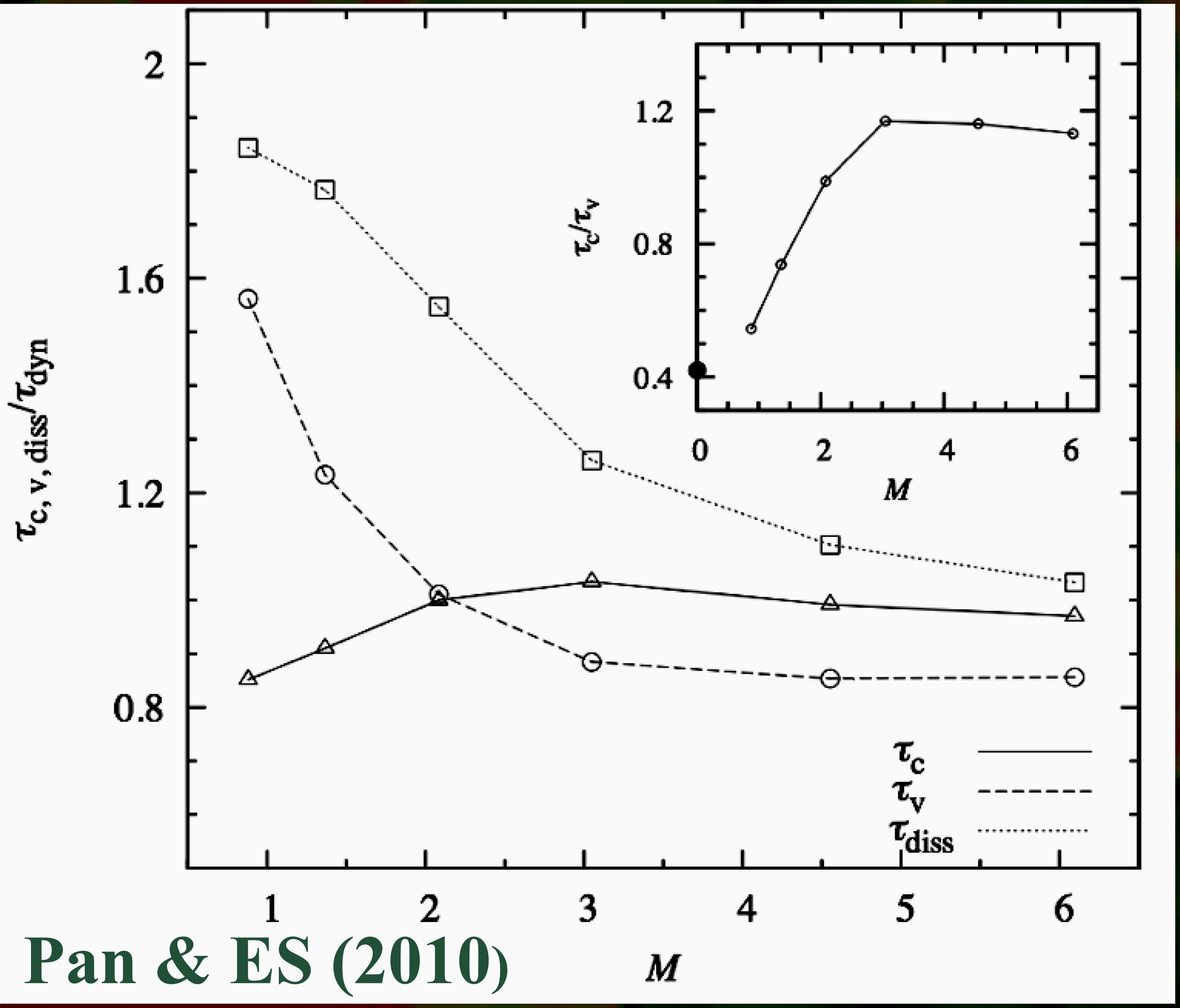

- Energy dissipation rate increases with M, shocks
- Mixing rate decreases with M compressible modes are less efficient at producing scalar structures at small scales

1. Kinetic energy contained in compressible modes first increases with M and then saturates at 1/3 for M>3, corresponding to equipartition.
2. pdV work has significant contribution (15-35%) to the conversion of kinetic energy to thermal energy.

2nd Order Velocity and Scalar Structure Functions

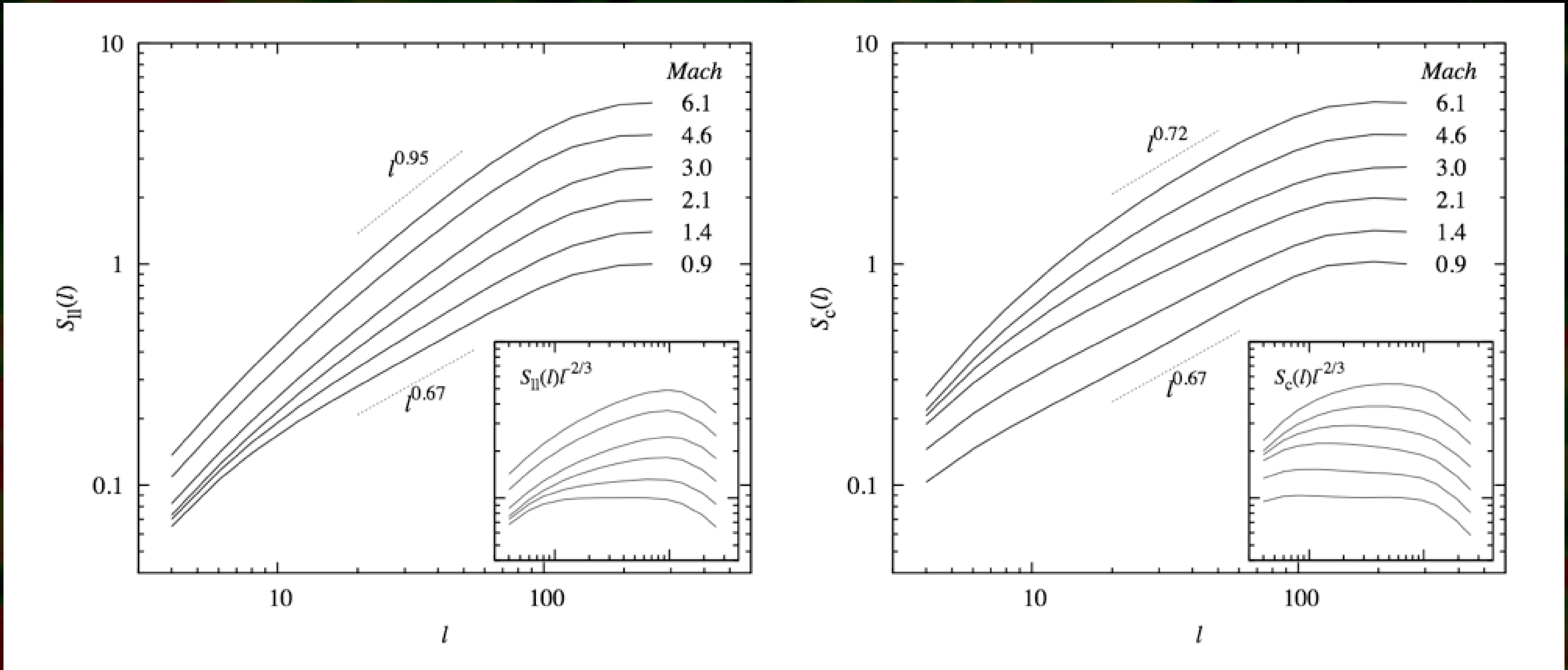

1. The velocity structure function steepens from 2/3 to 0.95 at M = 6.1, primarily due to increasing frequency and intensity of shocks

2. The slope of the scalar structure function first decreases from 2/3 at M=0.9 to 0.6 at M=2.1. However, at M >3, the slope starts to increase, due to the effect of strong compressible modes on scalar structures at large Mach numbers.

Pan & ES (2010)

High Order Velocity and Scalar Structure Functions

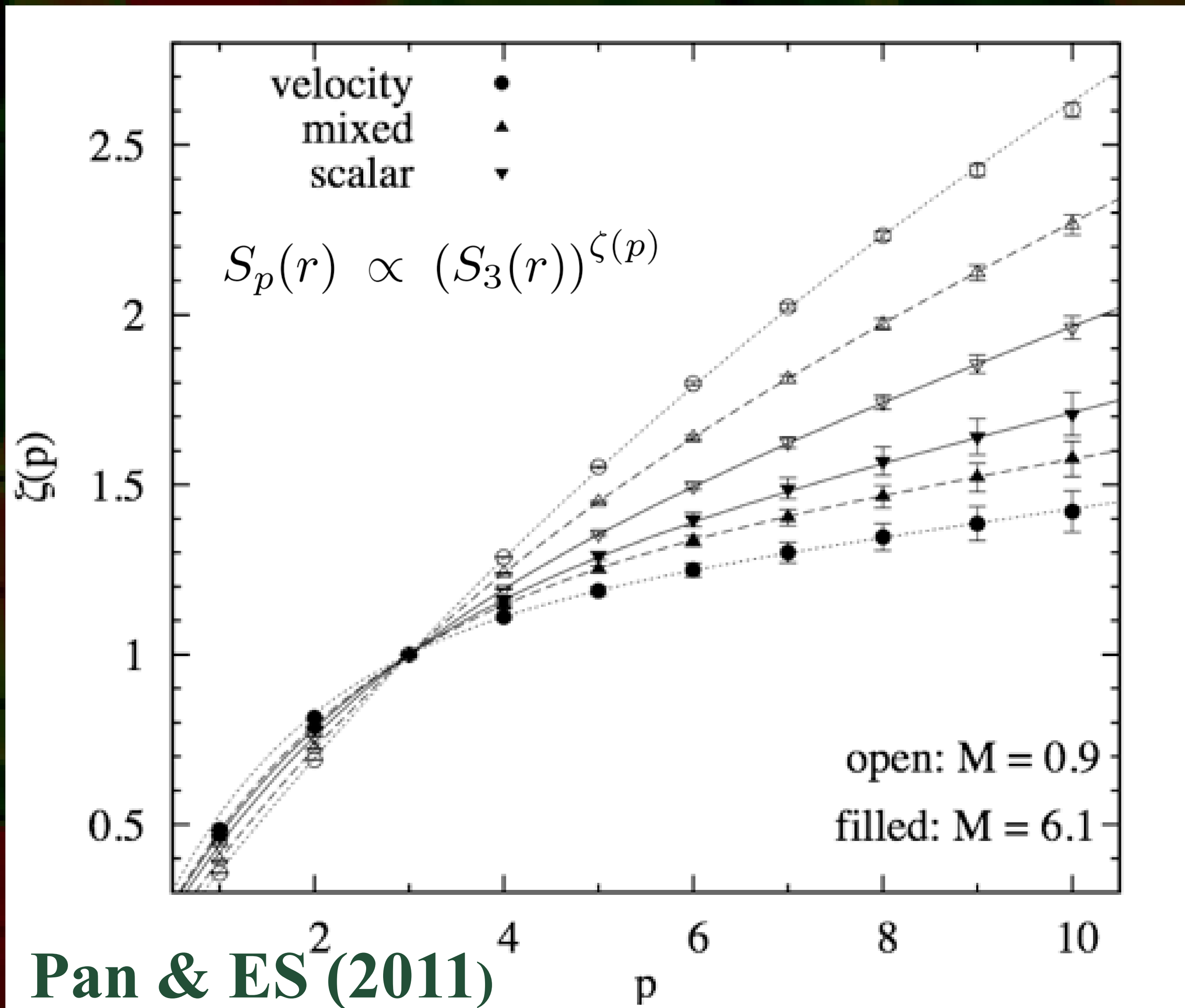

Pan & ES (2011)

Velocity: $$\left\langle |\delta v(r)|^p \right\rangle \propto r^{\xi_v(p)}$$

Mixed: $$\left\langle |\delta v(r)\delta C(r)^2|^{p/3} \right\rangle \propto r^{\xi_m(p)}$$

Scalar: $$\left\langle |\delta C(r)|^p \right\rangle \propto r^{\xi_c(p)}$$

where $$\delta v(r) \equiv v(x+r) - v(x)$$

and $$\delta C(r) \equiv C(x+r) - C(x)$$

incompressible flows show deviations from the Kolmogorov 1941 Scaling exponents in intermittency.

The intermittency model of She and Leveque (1994) is confirmed to be valid for all M, can use to measure fractal dimension.

The strongest velocity structures change from filamentary to sheet-like.

The most intense scalar structures are sheet-like at all Mach numbers.

Fluid Equations For Supersonic Turbulence

Thermal + Turbulent

$$\frac{\partial \rho u_i}{\partial t} + \frac{\partial \rho u_i u_j}{\partial x_j} = -\frac{\partial P}{\partial x_i}.$$

$$\frac{\partial \rho E}{\partial t} + \frac{\partial \rho E u_j}{\partial x_j} = \frac{\partial}{\partial x_j}\left(\mu_t \frac{\partial E}{\partial x_j}\right) - \frac{\partial P u_j}{\partial x_j} + \rho \dot{E}_{\mathrm{mech}}$$

$$\frac{\partial \rho F_r}{\partial t} + \frac{\partial \rho F_r u_j}{\partial x_j} = \frac{\partial}{\partial x_j}\left(\mu_t \frac{\partial F_r}{\partial x_j}\right),$$

ES & M. Bruggen (2009)

Fluid Equations For Supersonic Turbulence

K = Turbulent KE , L= Turbulent Length Scale

$$\frac{\partial \bar{\rho} K}{\partial t} + \frac{\partial \bar{\rho} K \tilde{u}_j}{\partial x_j} = \frac{\partial}{\partial x_j}\left(\mu_t \frac{\partial K}{\partial x_j}\right) - \frac{2}{3}\rho K \frac{\partial \tilde{u}_i}{\partial x_j} + \rho \dot{E}_{\rm mech} - \rho V C_D$$

turb. diffusion

$$\frac{\partial \bar{\rho} L}{\partial t} + \frac{\partial \bar{\rho} L \tilde{u}_j}{\partial x_j} = \frac{\partial}{\partial x_j}\left(\mu_t \frac{\partial L}{\partial x_j}\right) + C_C \bar{\rho} L \frac{\partial \tilde{u}_i}{\partial x_i},$$

turb. diffusion

growth of eddies through motion in mean flow

$$\mu_T = C_\mu \bar{\rho} L V, \qquad V \equiv \sqrt{2K}$$

turb. viscosity

turb. velocity

ES & M. Bruggen (2009)

initially hydrostatic galaxy, modeled after NGC 1569
4 levels of refinement, 39 parsec res., 25 X 25 x 30 kpc box
Atomic radiative cooling everywhere.
Star formation + supernovae according
to the empirical "Kennicutt Law"

Component	Parameter	Value
gas	a_{gas}	0.7 kpc
	b_{gas}	0.2 kpc
	M_{gas}	$2 \times 10^8 M_\odot$
	SFR	$0.17\ M_\odot/\mathrm{yr}$
	Z_{gas}	$0.25\ Z_\odot$
gas+stellar potential	a_{disk}	0.7 kpc
	b_{disk}	0.2 kpc
	M_{disk}	$3 \times 10^8 M_\odot$
DM halo	r_{DM}	2 kpc
	v_c	35 km/s

QuickTime™ and a decompressor are needed to see this picture.

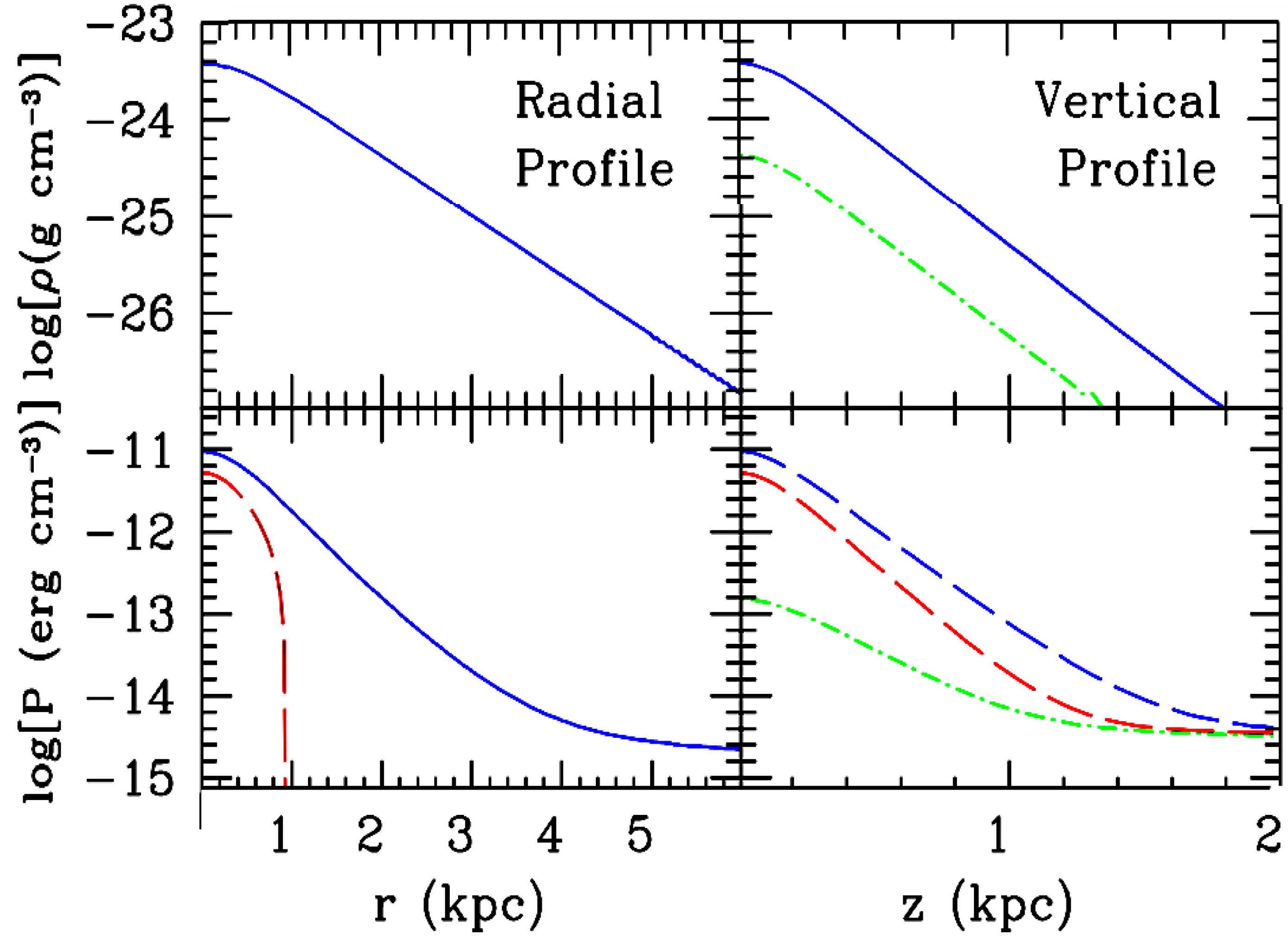

ES & M. Bruggen (2010)

$$\dot{E}_{\mathrm{mech}}$$

$$\Sigma_{\mathrm{SFR}} = 2.5 \times 10^{-4} \frac{M_\odot}{\mathrm{yr\,kpc^2}} \left(\frac{\Sigma_{\mathrm{gas}}}{10^6 M_\odot \mathrm{kpc}^{-2}} \right)^{1.5}$$

1 SN per 150 $M_\odot$

All K, $L = R_{bubble}$

$M_z = 2\, M_\odot$ per SN

ES & M. Bruggen (2010)

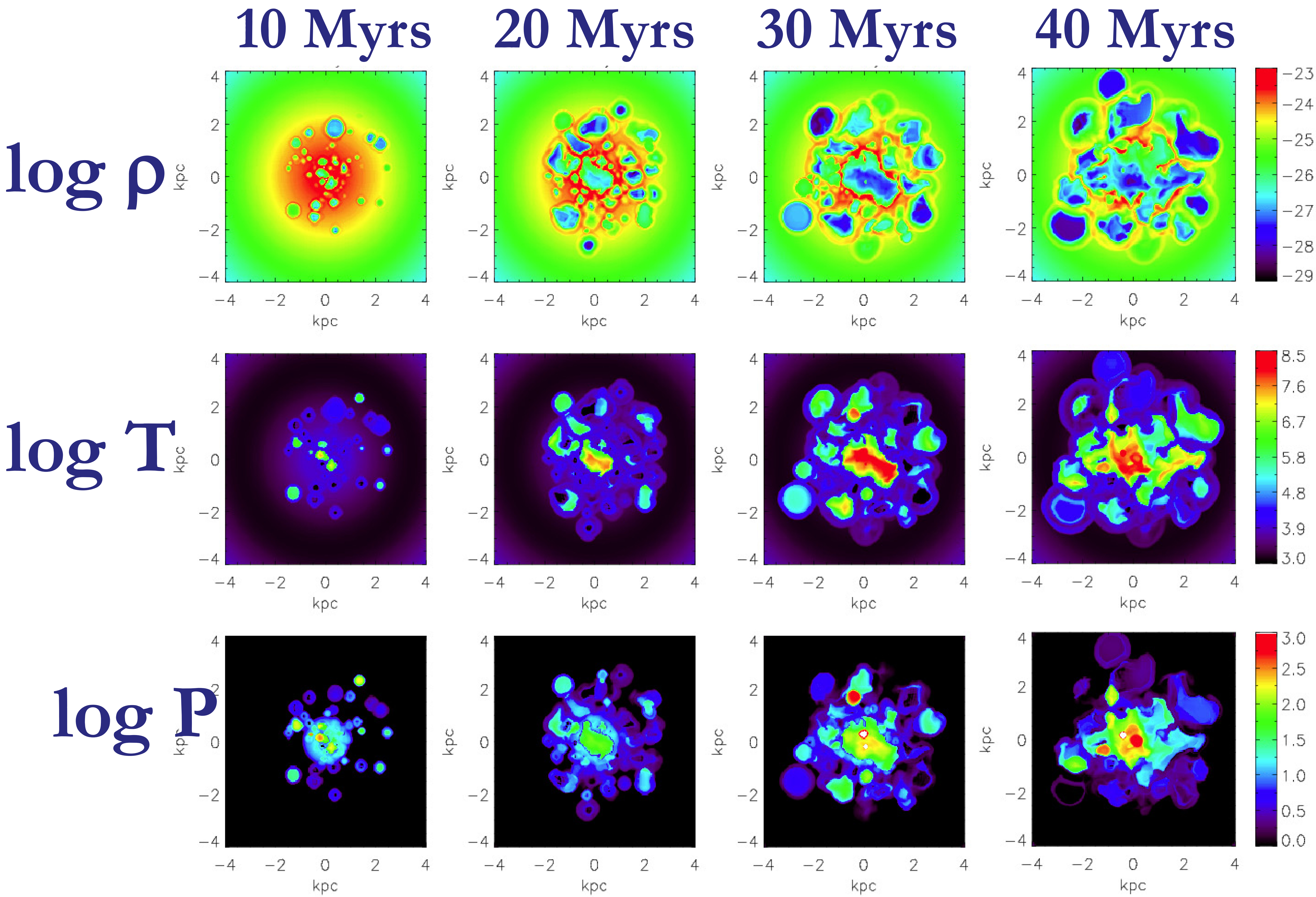

ES & M. Bruggen (2010)

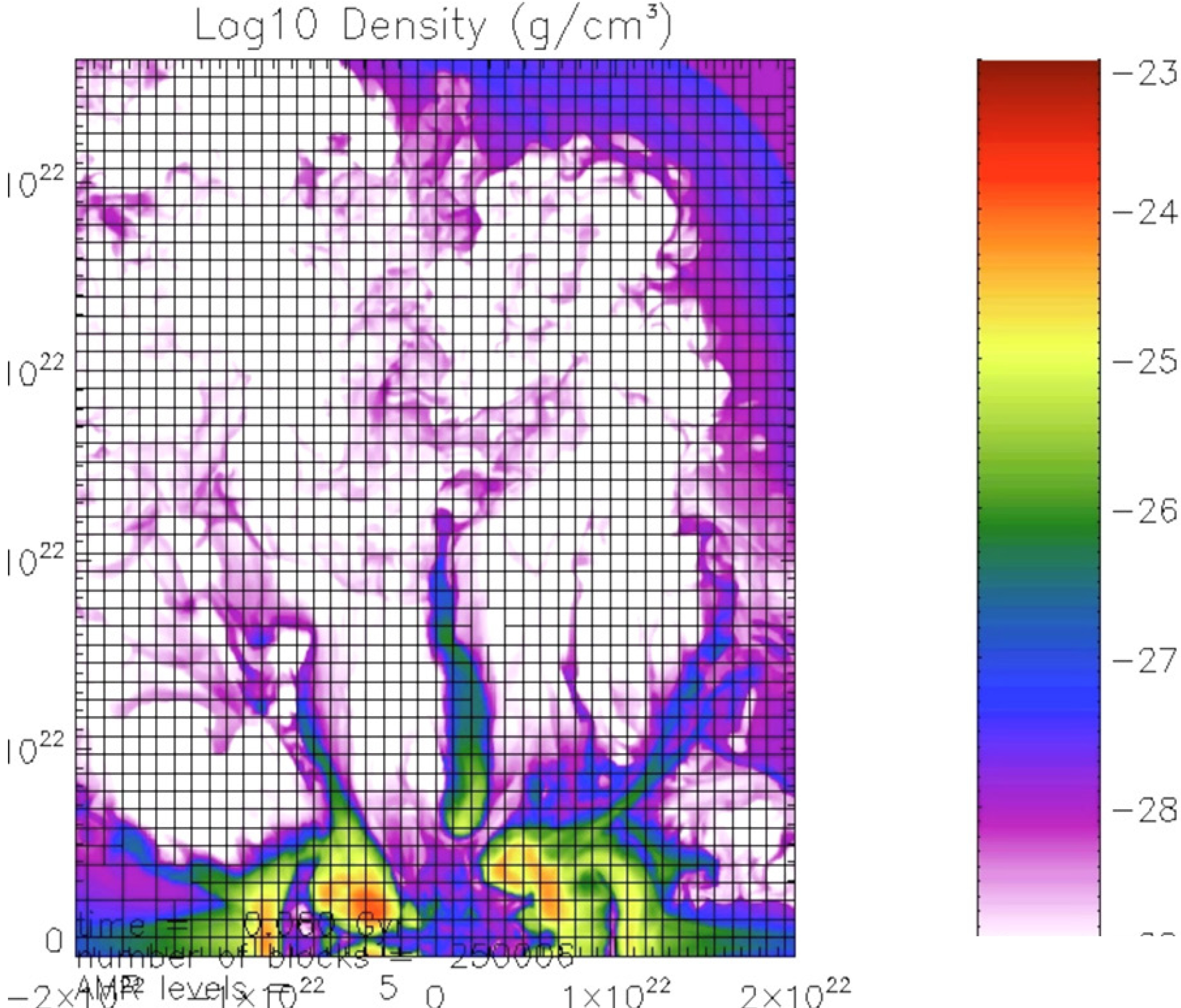

Log10 Density (g/cm³)
10^{22}
10^{22}
10^{22}
10^{22}
0
time = 0.060 Gyr
number of blocks = 250006
AMR levels = 5
-2×10^{22}
-1×10^{22}
0
1×10^{22}
2×10^{22}
−23
−24
−25
−26
−27
−28

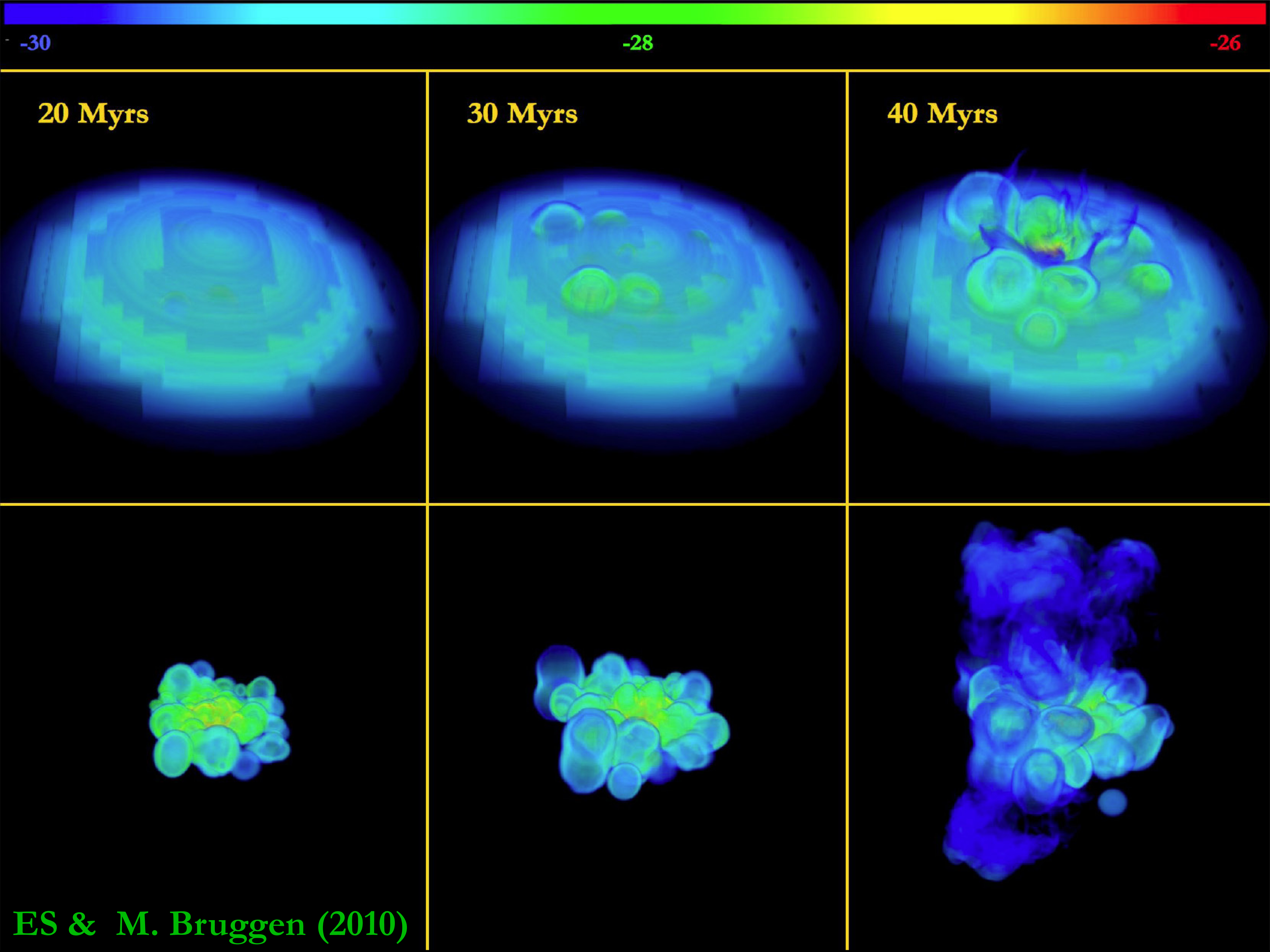
-30
-28
-26
20 Myrs
30 Myrs
40 Myrs
ES & M. Bruggen (2010)

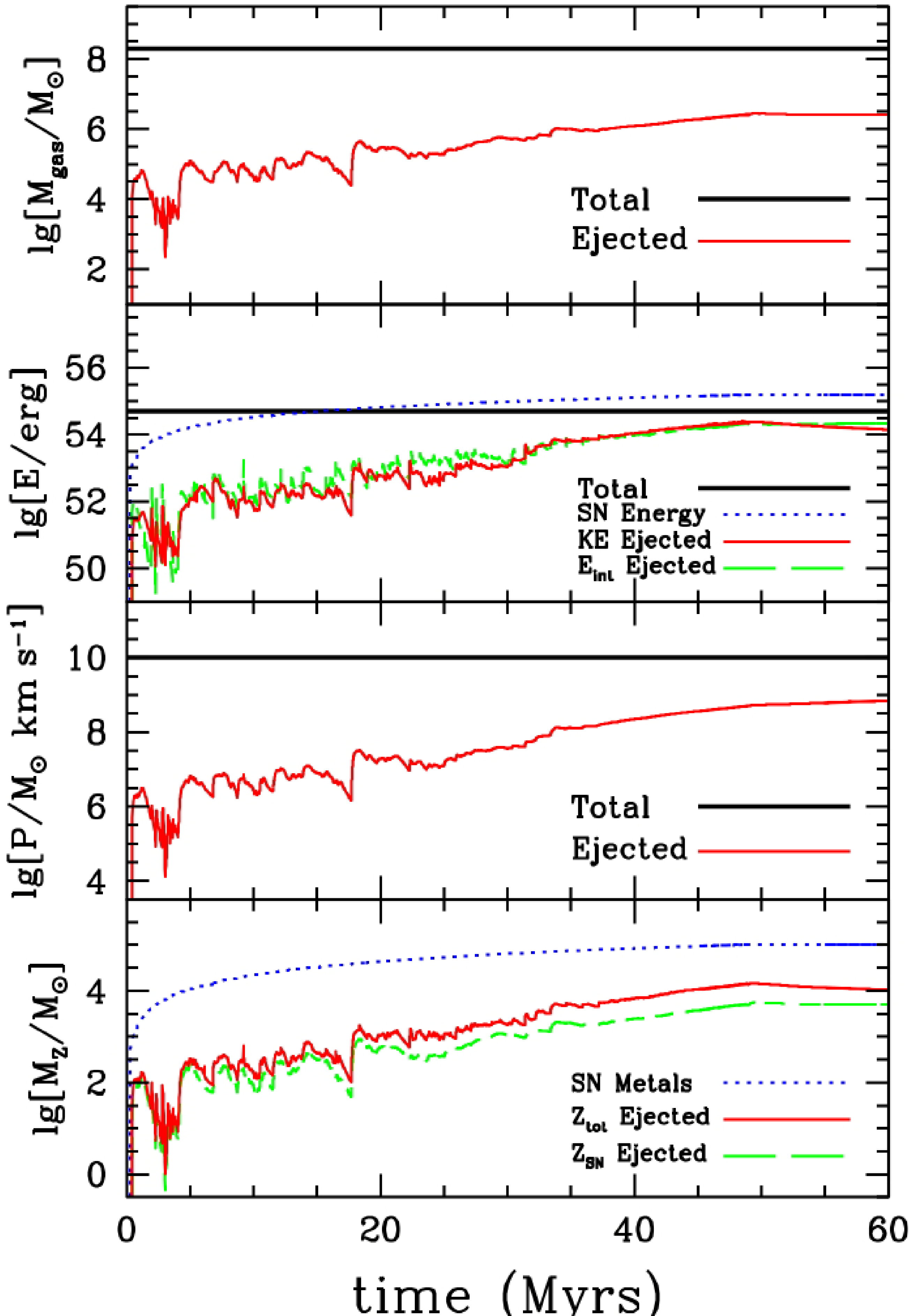

$M_\star = 8\times10^6 M_\odot$

$\approx 8\times10^6 M_{Ej}$

$E_{SN} < E_{total\text{-}ej}$

$V_{ej} \approx 50$ km/s

ES & M. Bruggen (2010)

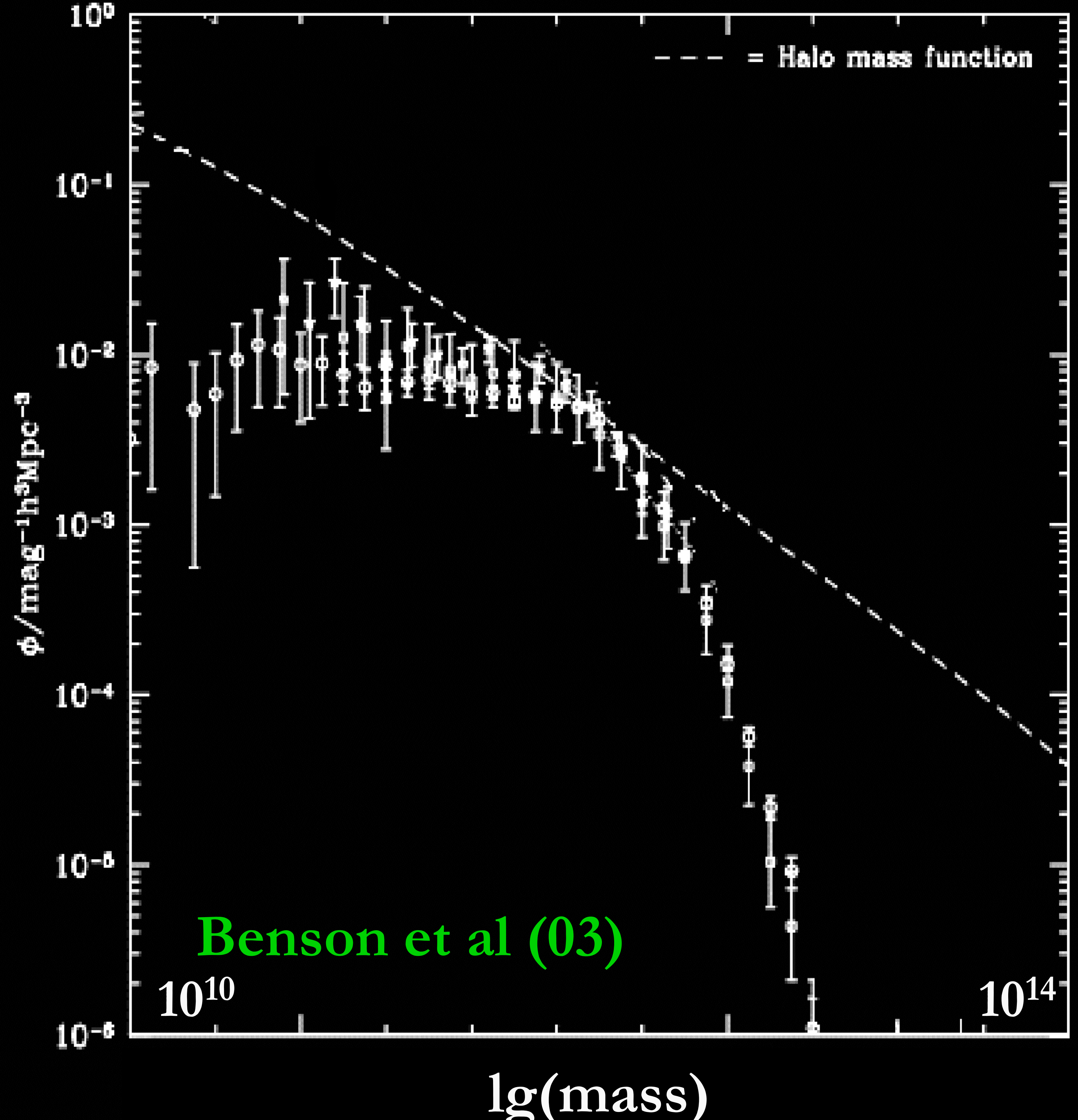

- - - = Halo mass function
10^0
10^{-1}
10^{-2}
10^{-3}
10^{-4}
10^{-5}
10^{-6}
φ/mag⁻¹h³Mpc⁻³
Benson et al (03)
10^{10}
10^{14}
lg(mass)

II High Mass Feedback

Fabian et al (2006)

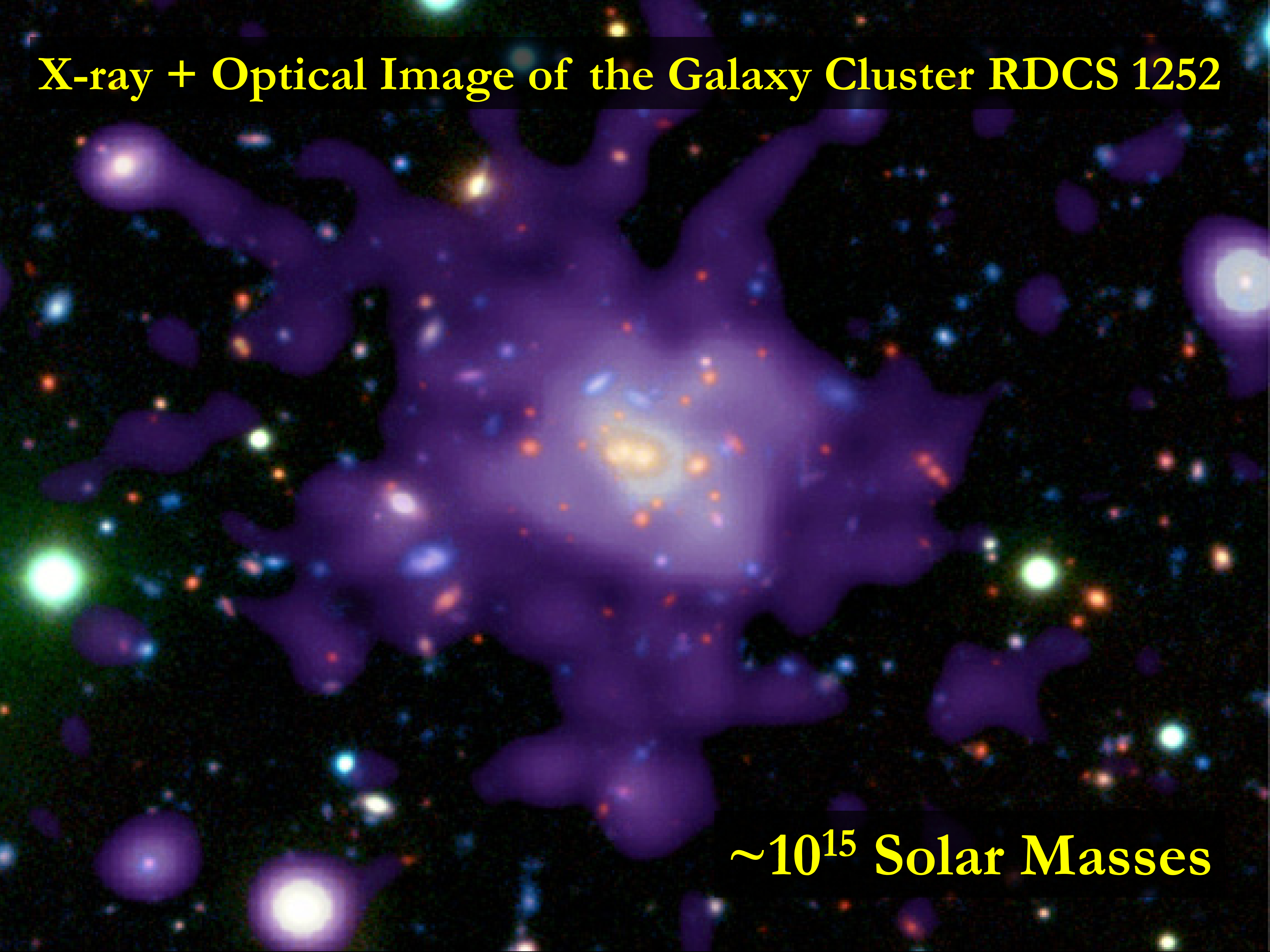
X-ray + Optical Image of the Galaxy Cluster RDCS 1252
~10^15 Solar Masses

X-ray Image of the Perseus Galaxy Cluster

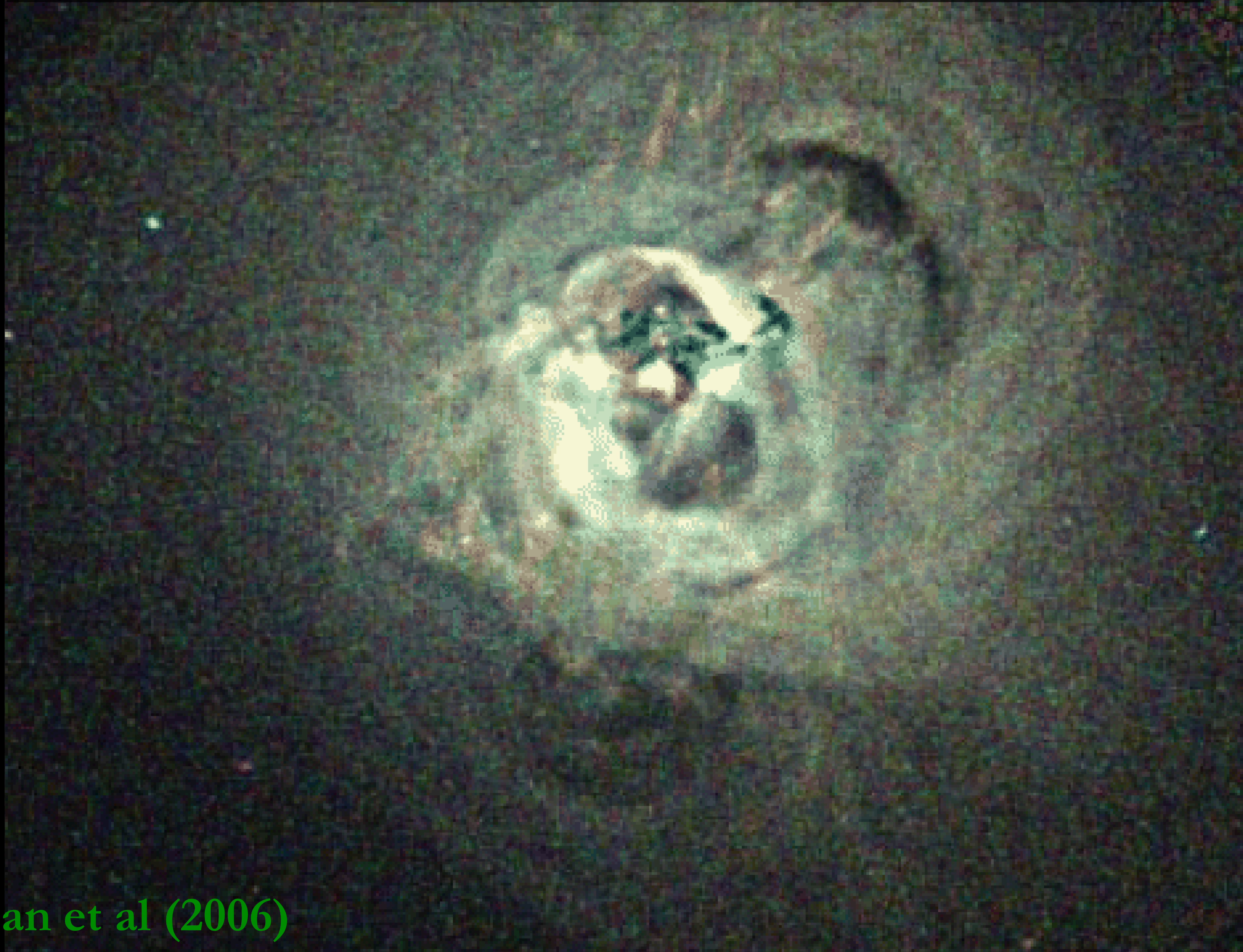

Fabian et al (2006)

Rayleigh Taylor Instability

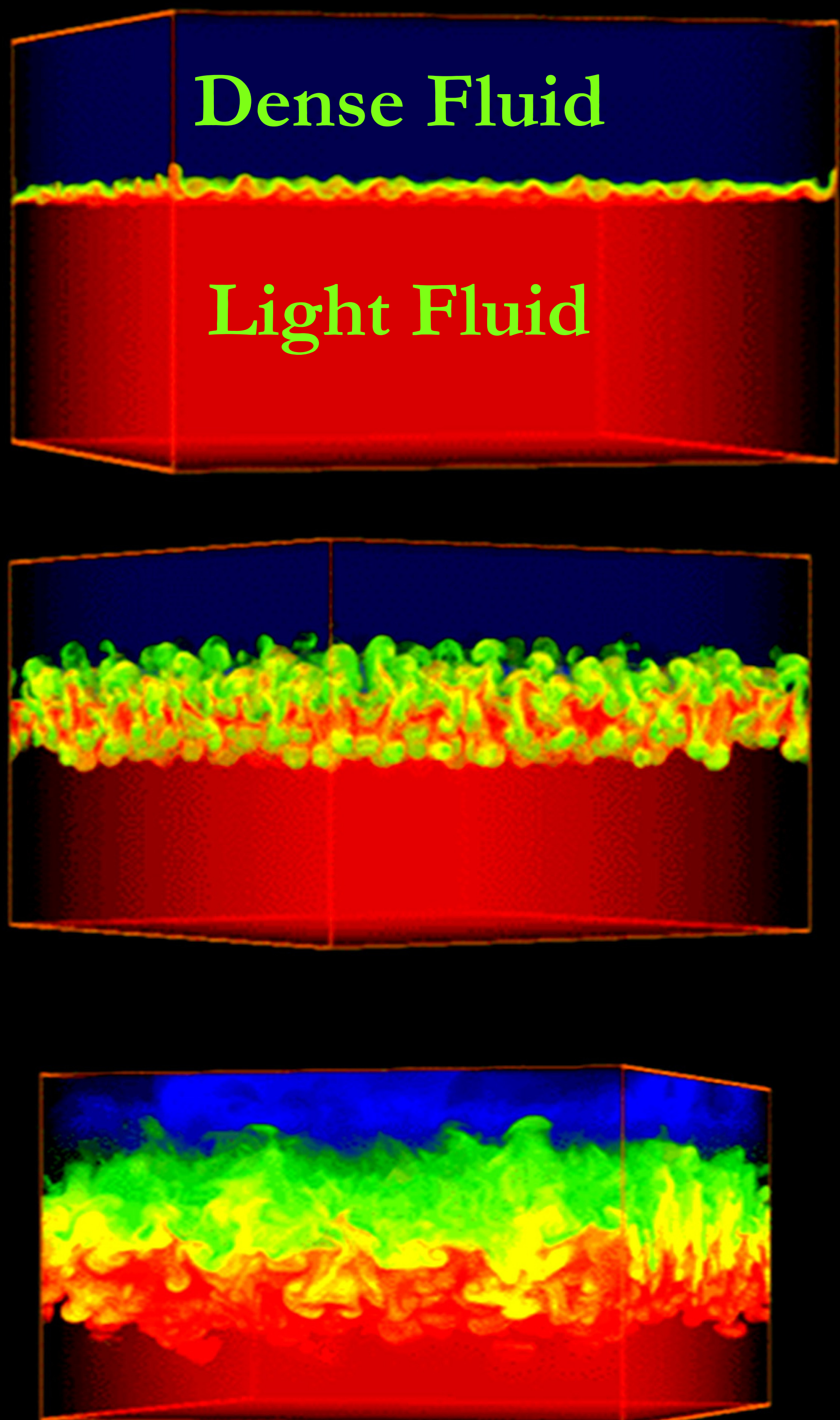

$$h_b = \alpha_b A_o g t^2$$

$$A_i = \frac{\bar{\rho}_+ - \bar{\rho}_-}{\bar{\rho}_+ + \bar{\rho}_-}.$$

$$\lambda_{\max} = 4\,\pi\,(\nu^2\,A/g)^{1/3}$$

Ionized Medium

$\text{viscosity} \propto V_i \lambda_i$ V_i = Velocity of ions

$$\lambda_i = 1/[n\,\pi\,(e^2/3kT)^2$$

Spitzer $\nu \approx 20\ \text{kpc} \times 1000\ \text{km/s}\ n_{-3}^{-1}\, T_8^{5/2}$

viscous bubble evolution

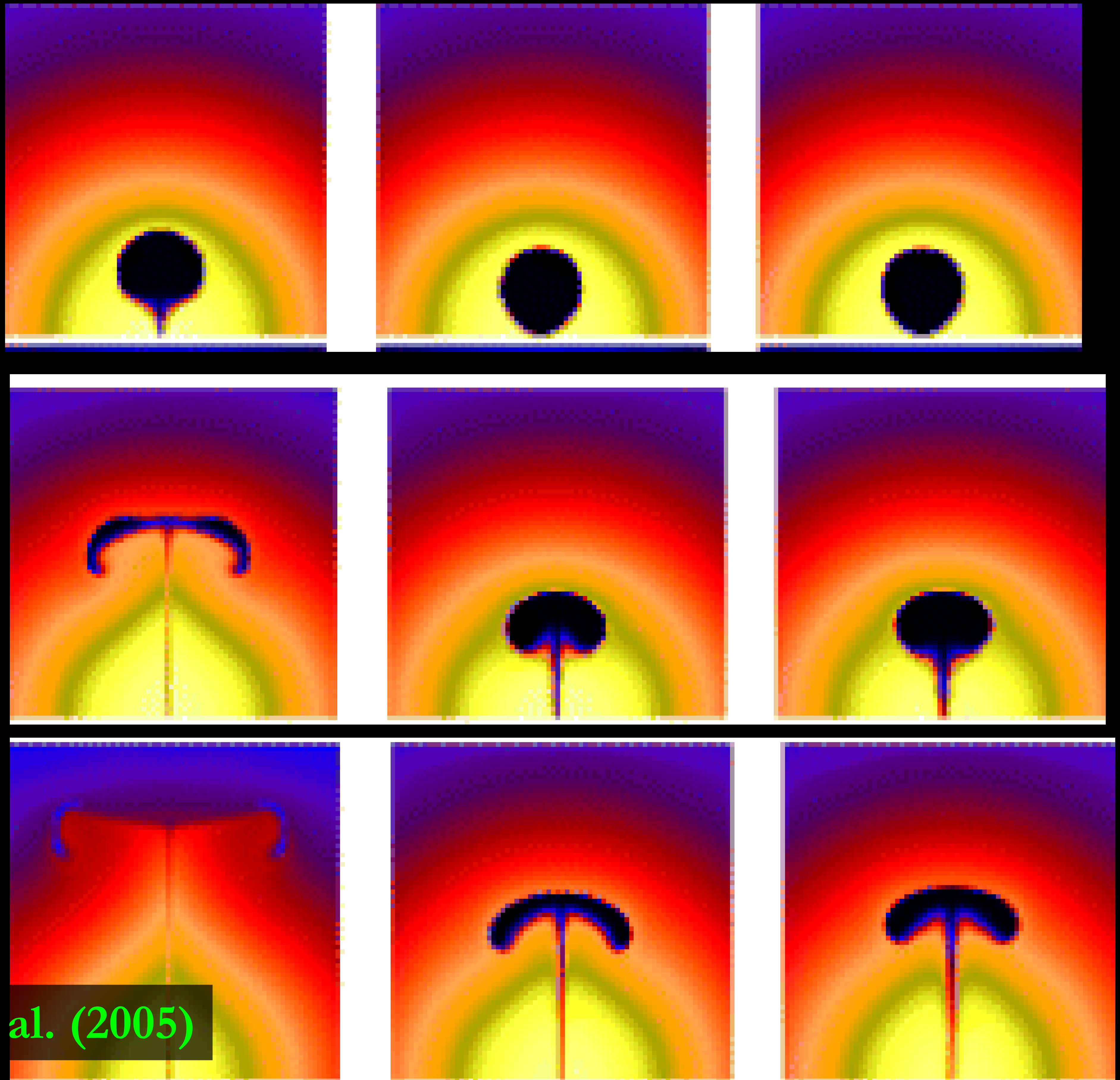

Reynolds et al. (2005)

Ionized Medium

viscosity $\propto V_i \lambda_i$ V_i = Velocity of ions

$$\lambda_i = 1/[n\,\pi\,(e^2/3kT)^2$$

$$\nu \approx 20 \text{ kpc} \times 1000 \text{ km/s } n_{-3}^{-1} T_8^{5/2}$$

$$\lambda_{I,B} = (m\, v_i / eB)$$

$$\nu \approx 10^{10} \text{ cm } (T_8^{1/2}/B_{\mu G}) \times 1000 \text{ km/s } T_8^{1/2}$$

Simulation setup

FLASH3.0, AMR

initially hydrostatic cluster, modeled after Perseus, static gravity

5 levels of refinement (3-6), 1024^3 eff. res., (650 kpc)^3 box

radiative cooling by thermal bremsstrahlung

bubbles are produced by injection of energy into spherical regions

Saguaro cluster (4096core cluster at ASU)

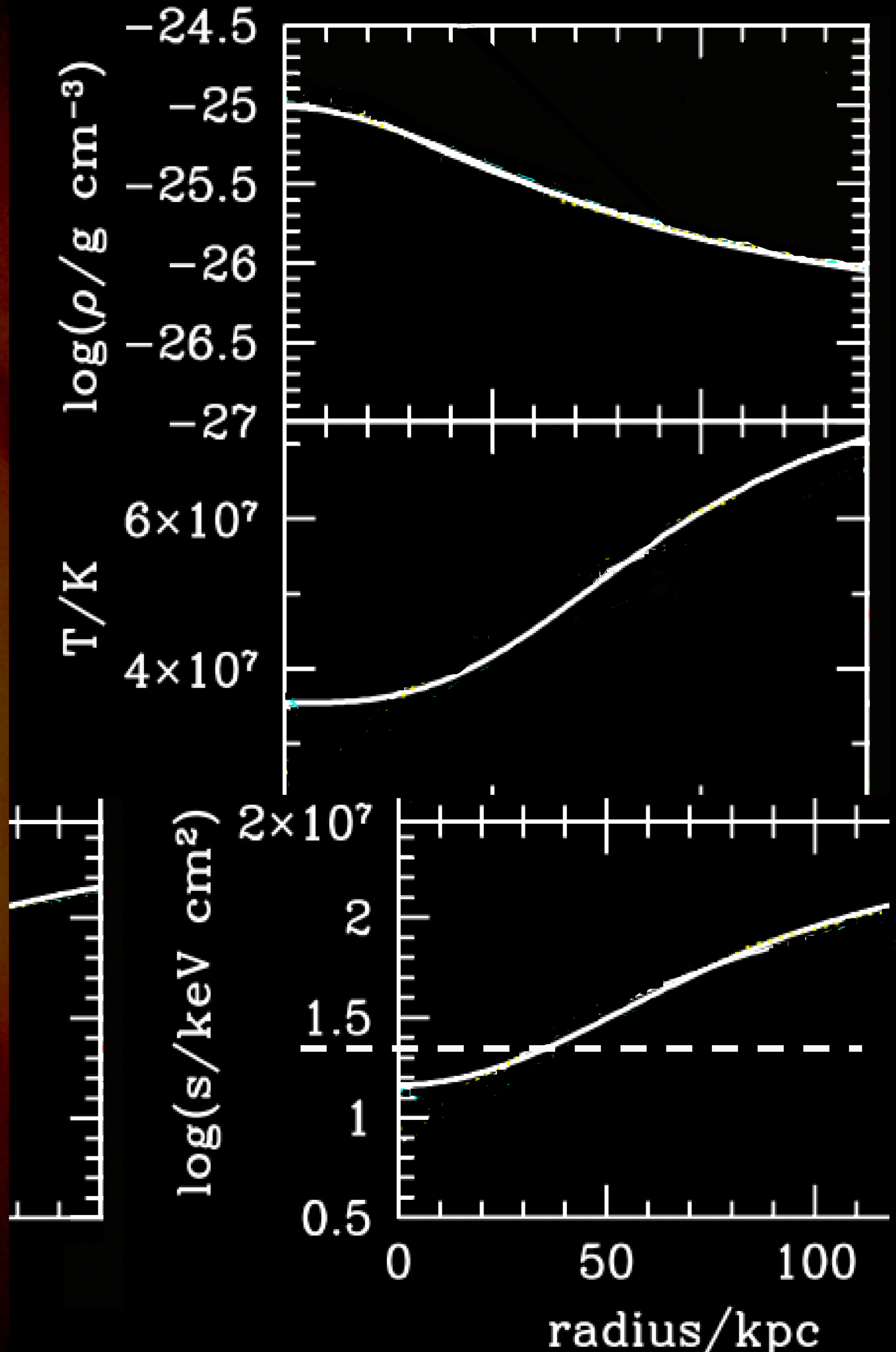

ES and M. Bruggen (2008)

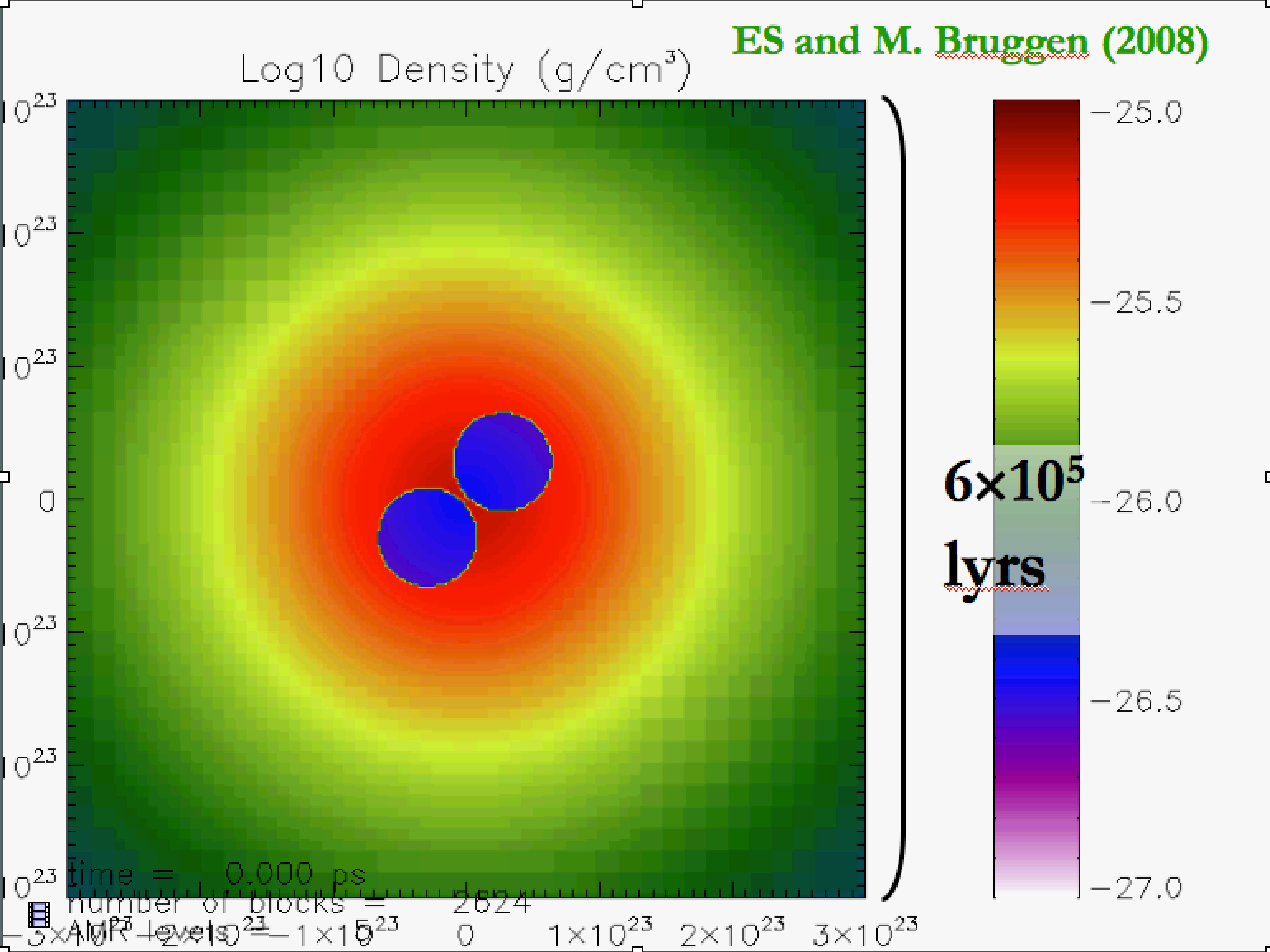
ES and M. Bruggen (2008)
Log10 Density (g/cm³)
6×10⁵
lyrs
−25.0
−25.5
−26.0
−26.5
−27.0
0
time = 0.000 ps
number of blocks = 2624
AMR levels
1×10²³
2×10²³
3×10²³

ES and M. Bruggen (2008)

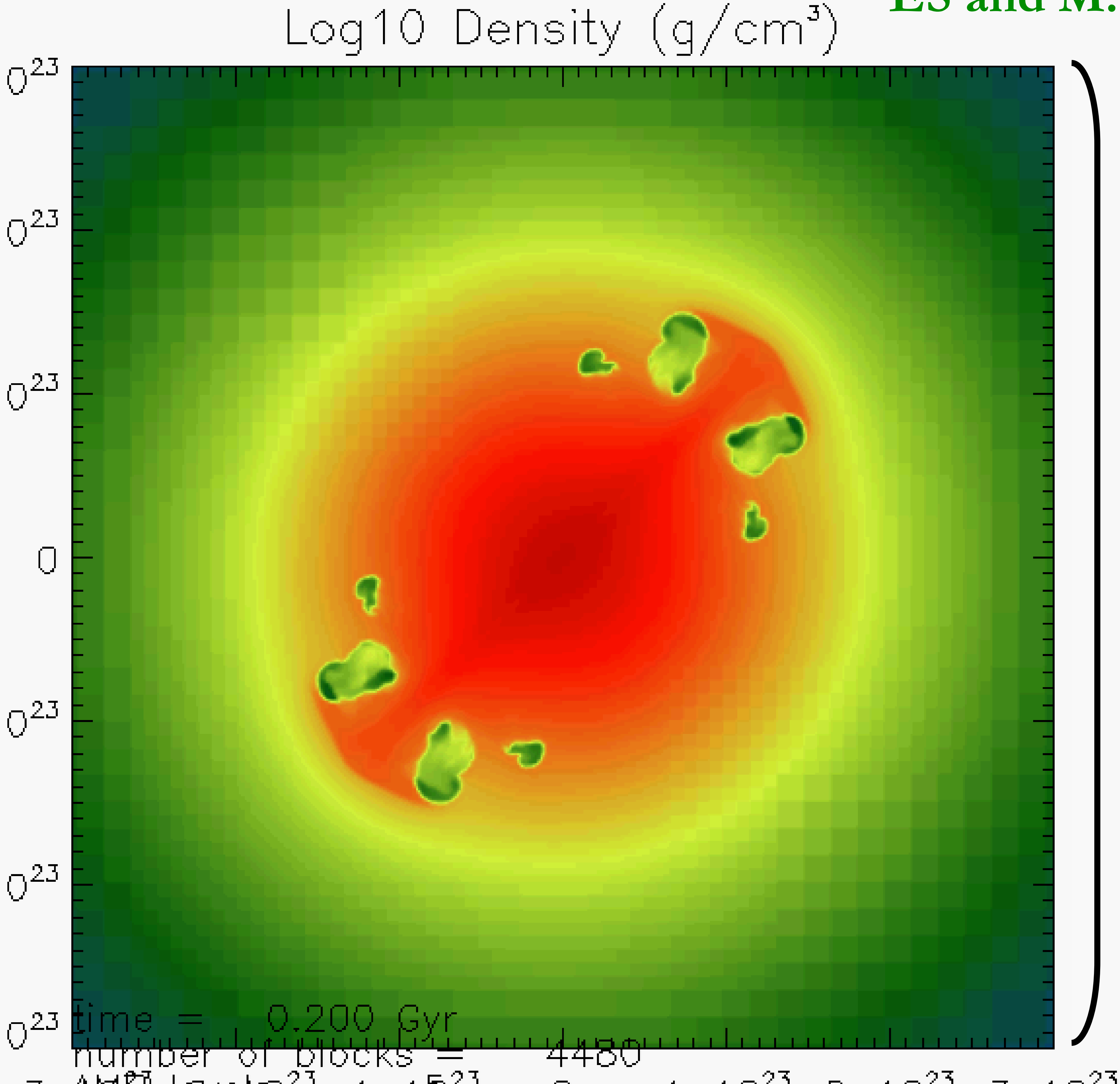

6×10^5 lyrs

SEE ALSO:
Robinson et al '05
Reynolds et al '05
Bruggen '05

Dependence on Resolution $\lambda_{\max} = 4\pi(\nu^2 A/g)^{1/3}$

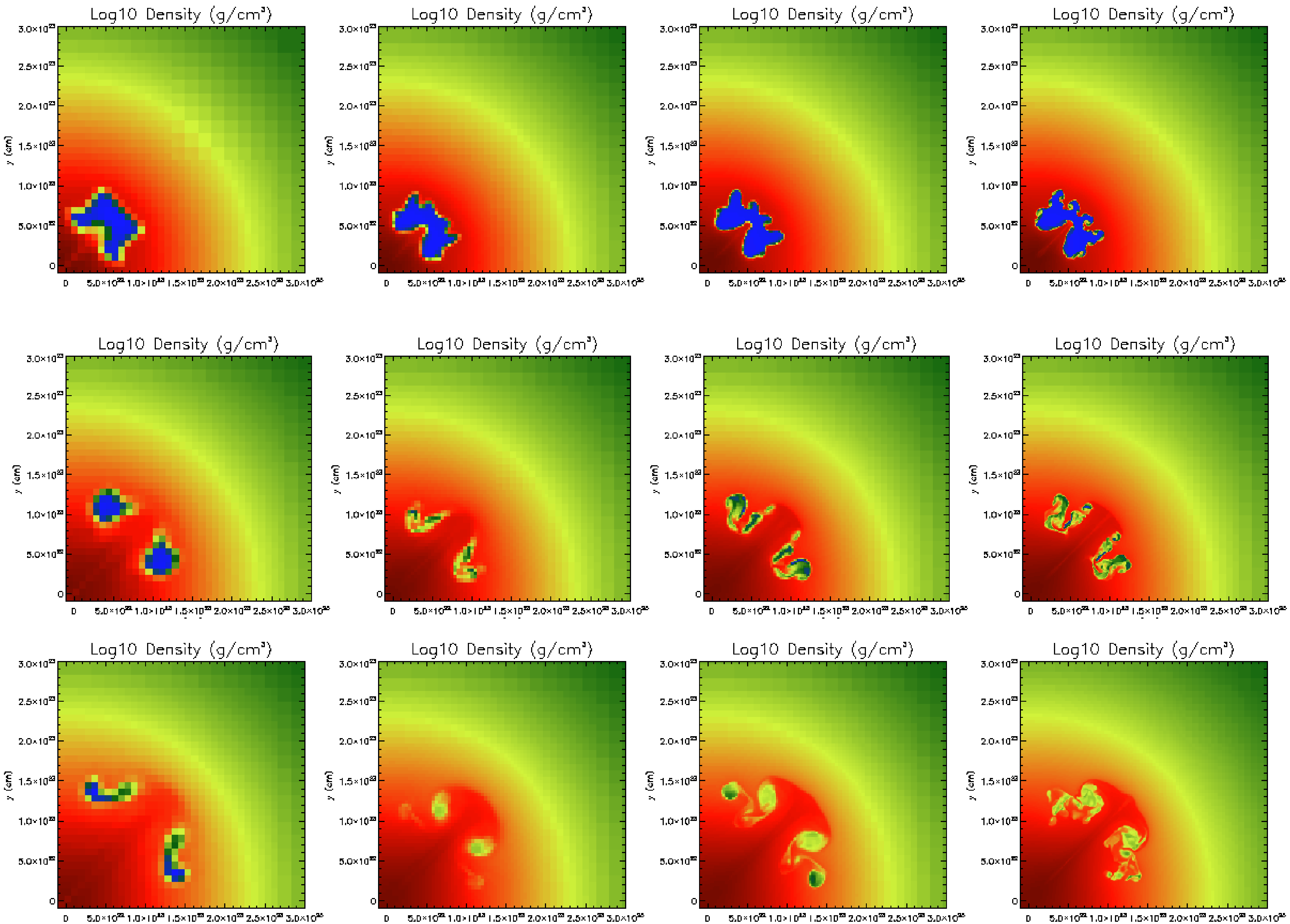

ES and M. Bruggen (2008)

X-ray Image of the Perseus Galaxy Cluster

Fabian et al (2006)

Dimonte & Tipton '06 Turbulence Model

based on buoyancy-drag models for RT and RM instabilities: **self-similar, conserves energy, preserves Galilean invariance, works with shocks**

K = Turbulent KE , L= Turbulent Length Scale

$$\frac{\partial \bar{\rho} K}{\partial t} + \frac{\partial \bar{\rho} K \tilde{u}_j}{\partial x_j} = \frac{\partial}{\partial x_j}\left(\frac{\mu_t}{N_K}\frac{\partial K}{\partial x_j}\right) - \frac{2}{3}\rho K \frac{\partial \tilde{u}_i}{\partial x_j} + S_K$$

turb. diffusion

work associated with turbulent stress

source term with RM and RT contributions

$$\frac{\partial \bar{\rho} L}{\partial t} + \frac{\partial \bar{\rho} L \tilde{u}_j}{\partial x_j} = \frac{\partial}{\partial x_j}\left(\mu_t \frac{\partial L}{\partial x_j}\right) + \bar{\rho} V + C_C \bar{\rho} L \frac{\partial \tilde{u}_i}{\partial x_i},$$

turb. diffusion

growth of eddies through turb. motion

growth of eddies through motion in mean flow

$$S_K = \bar{\rho} V \left[C_B A_i g_i - C_D \frac{V^2}{L} \right], \qquad \mu_T = C_\mu \bar{\rho} L V, \qquad V \equiv \sqrt{2K}$$

buoyancy

drag

turb. viscosity

turb. velocity

Rayleigh-Taylor Shock Tube Test

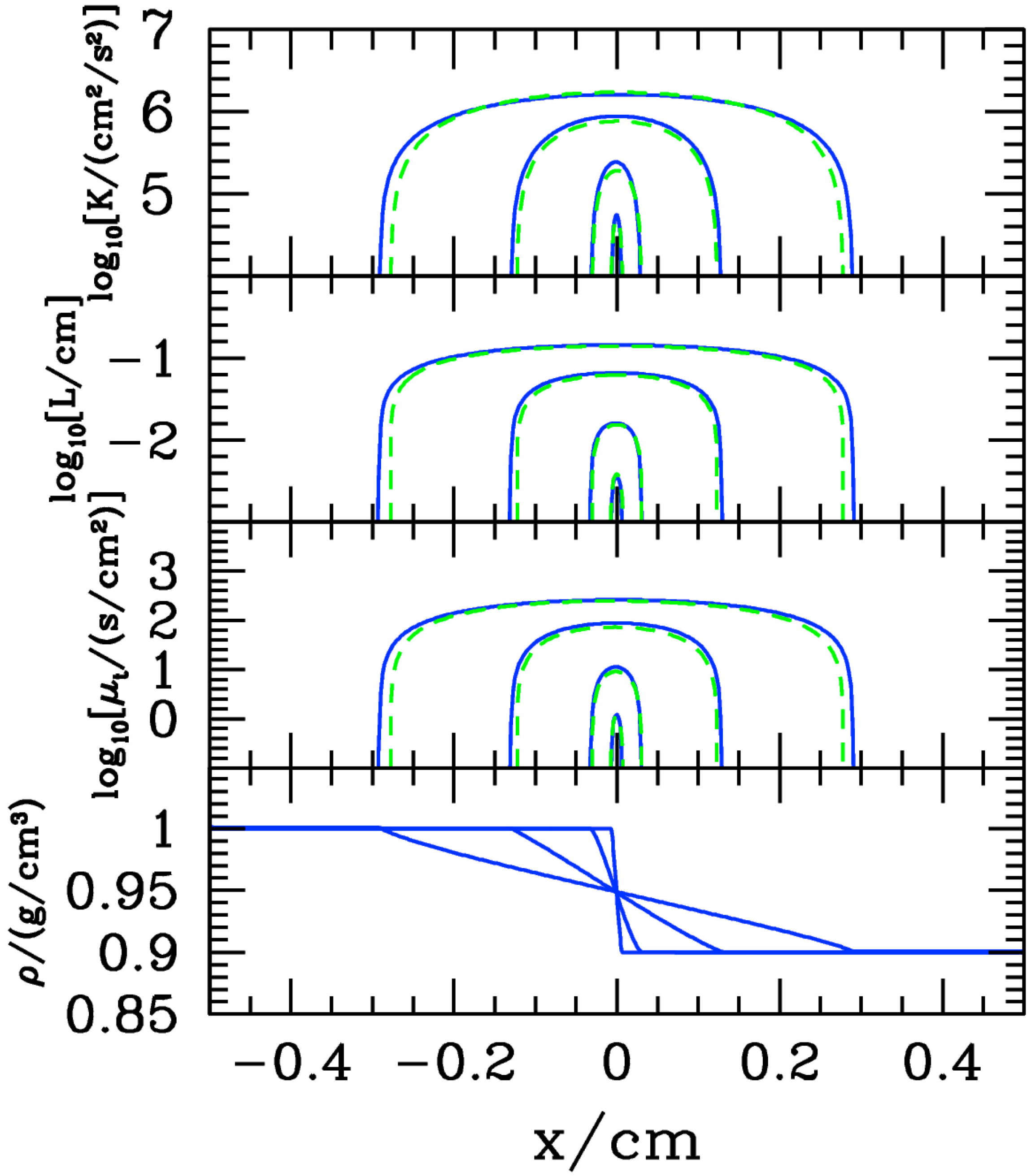

solid: simulation
dashed: analytic

$$L(x,t) = L(t,0)[1 - x^2/h(t)^2]^{1/2}$$

$$K(x,t) = K(t,0)[1 - x^2/h(t)^2]$$

$$h(t) = \alpha A(0) t^2$$

$$L(t,0) = h(t)/2$$

$$K(t,0) = (dh/dt)^2/2$$

ES and M. Bruggen (2008)

ES and M. Bruggen (2008)

6×10^5

lyrs

ES and M. Bruggen (2008)

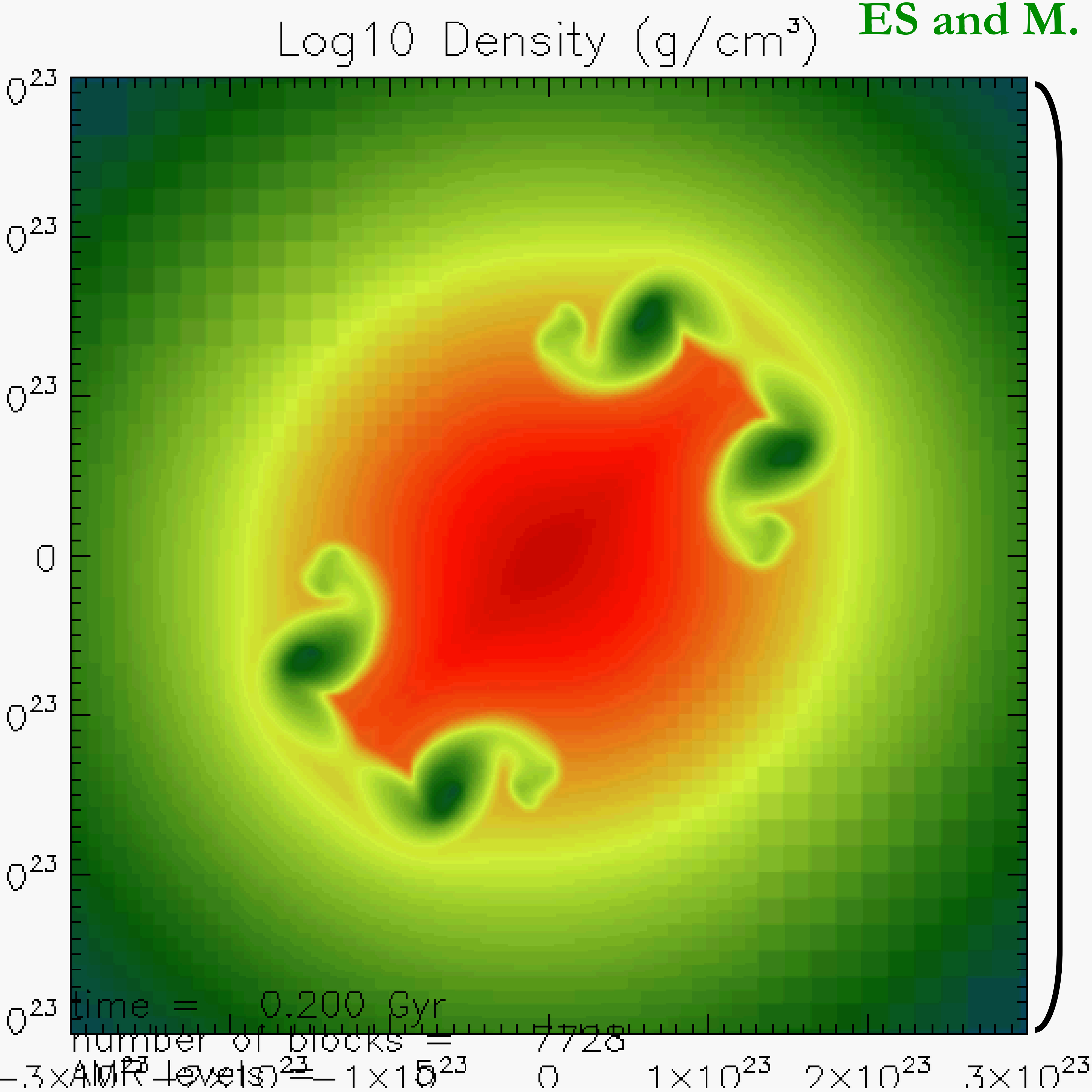

6×10⁵ lyrs

Dependence on Resolution $\lambda_{\max} = 4\pi(\nu^2 A/g)^{1/3}$

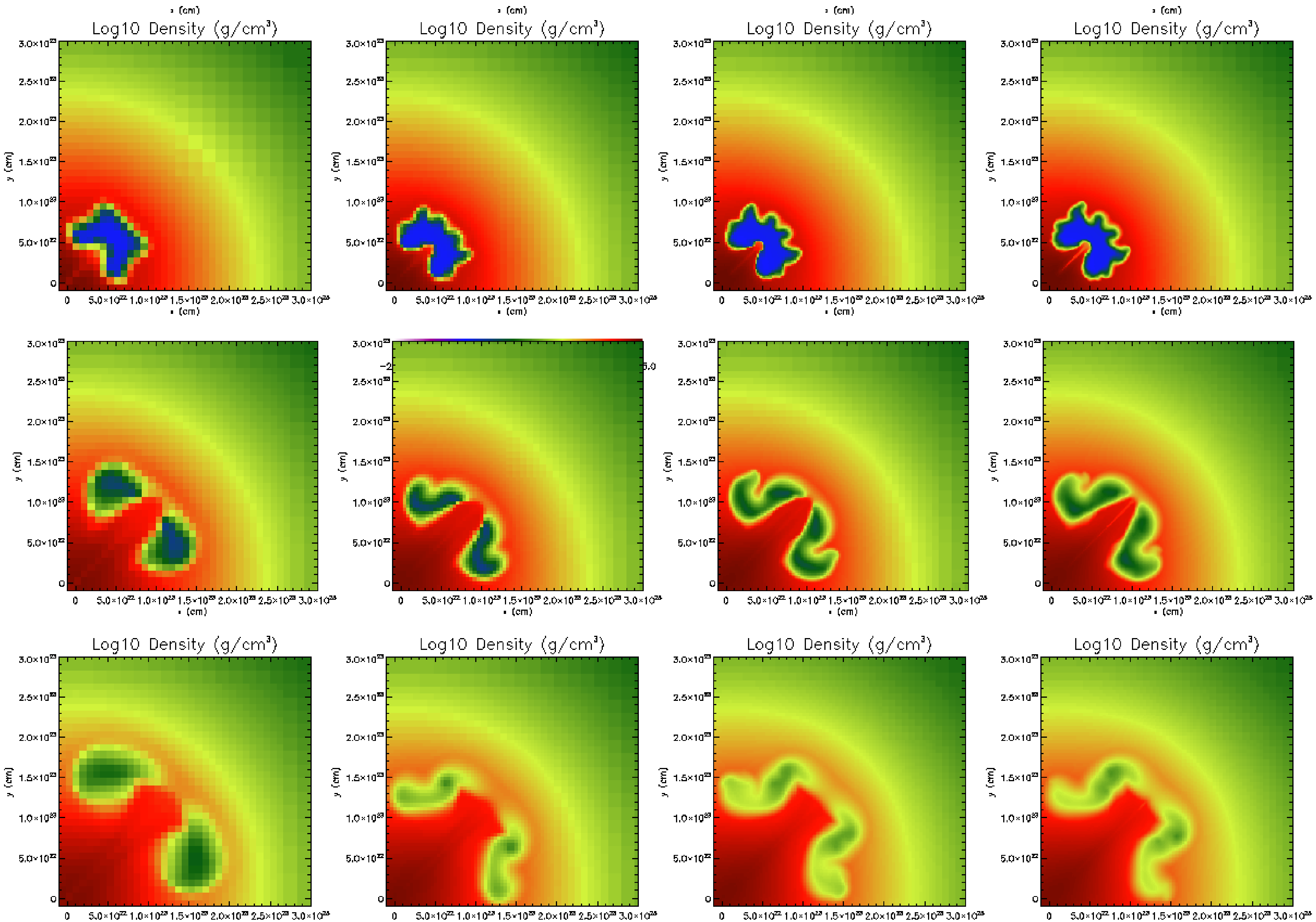

ES and M. Bruggen (2008)

Dependence on Resolution

$$\lambda_{\max} = 4\pi(\nu^2 A/g)^{1/3}$$

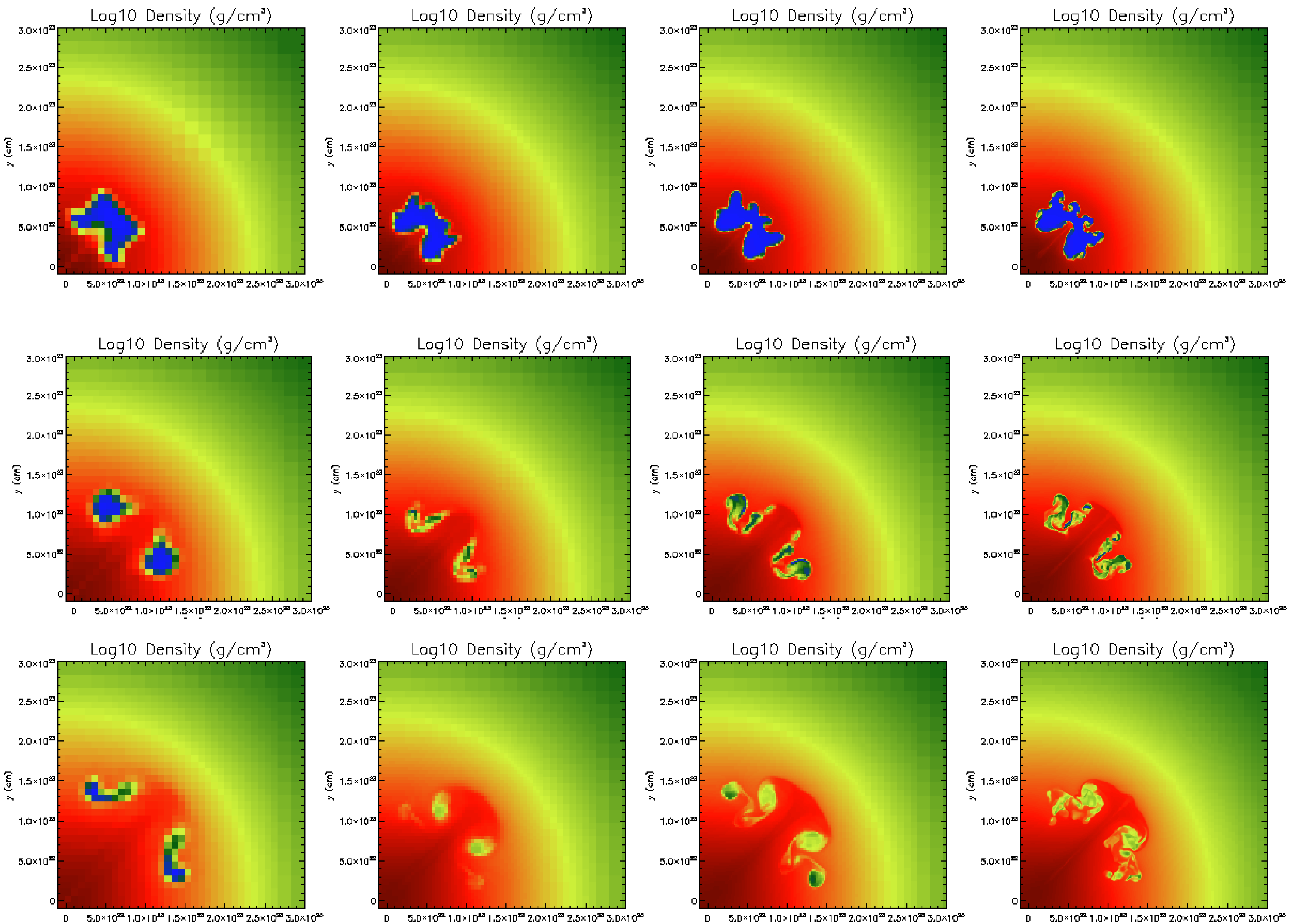

ES and M. Bruggen (2008)

Density Slices X-ray

50 Myrs

100 Myrs

150 Myrs

No Turb. Turbulence No Turb. Turbulence

ES and M. Bruggen (2008)

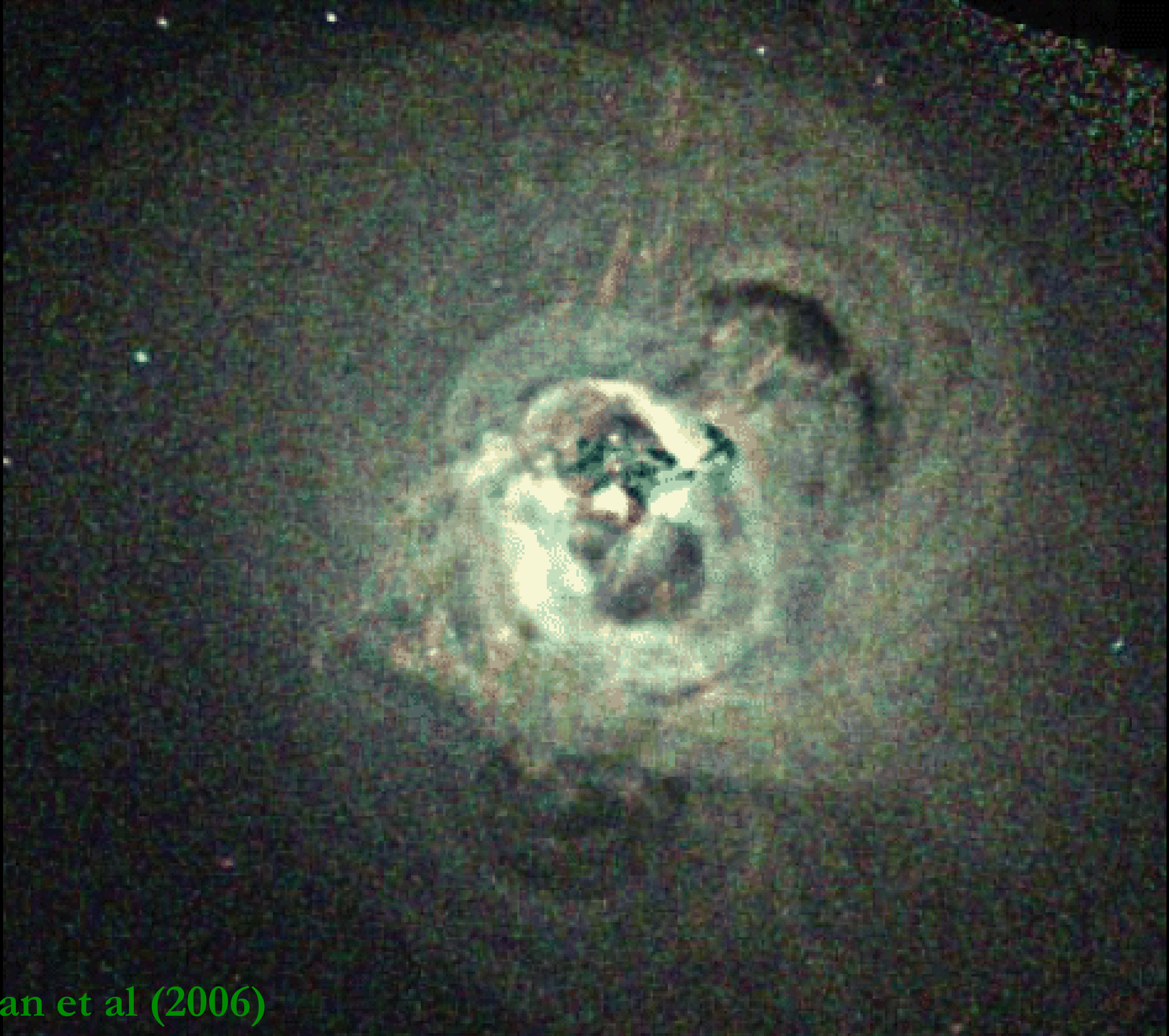

Fabian et al (2006)

ES and M. Bruggen (2008)

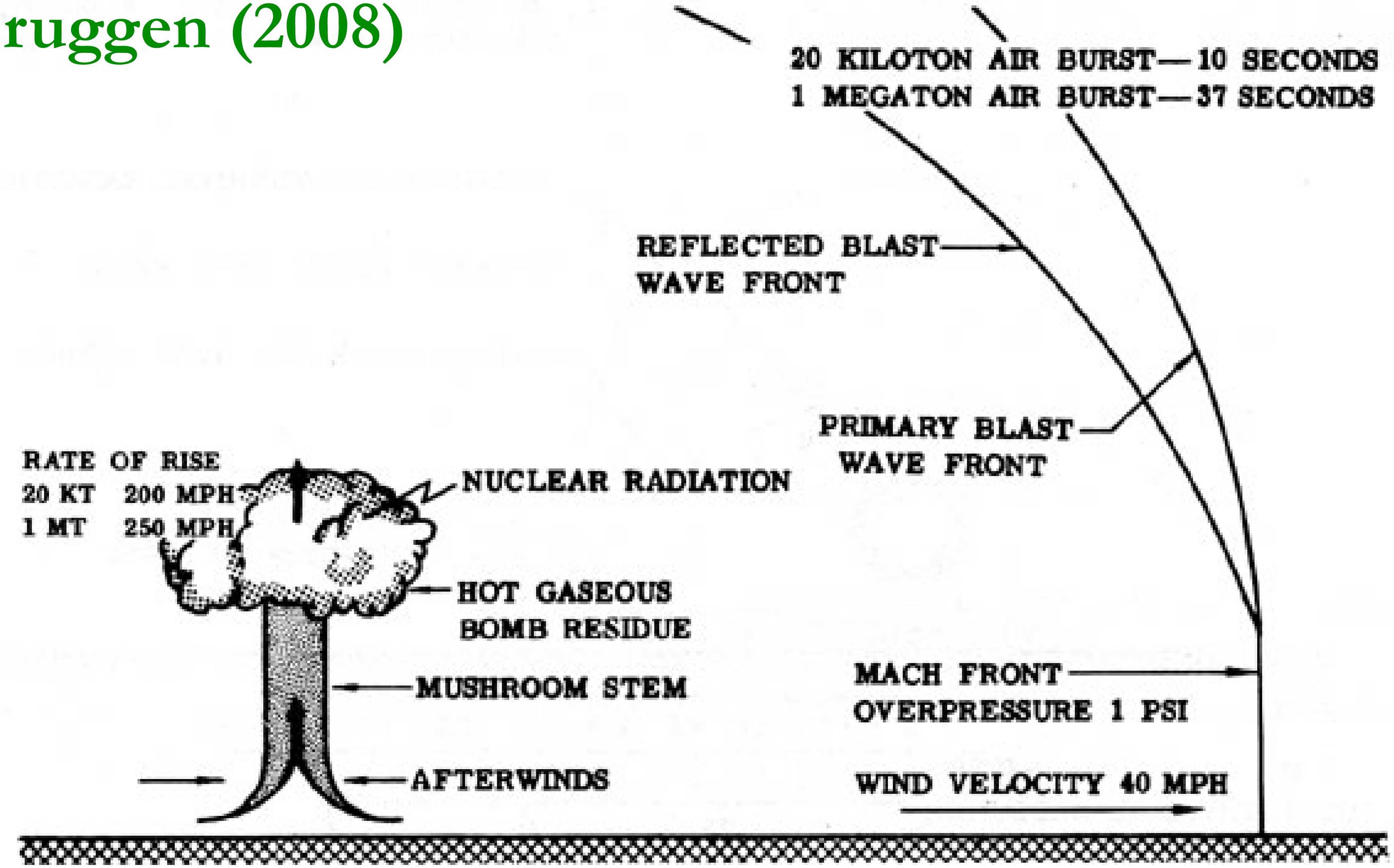

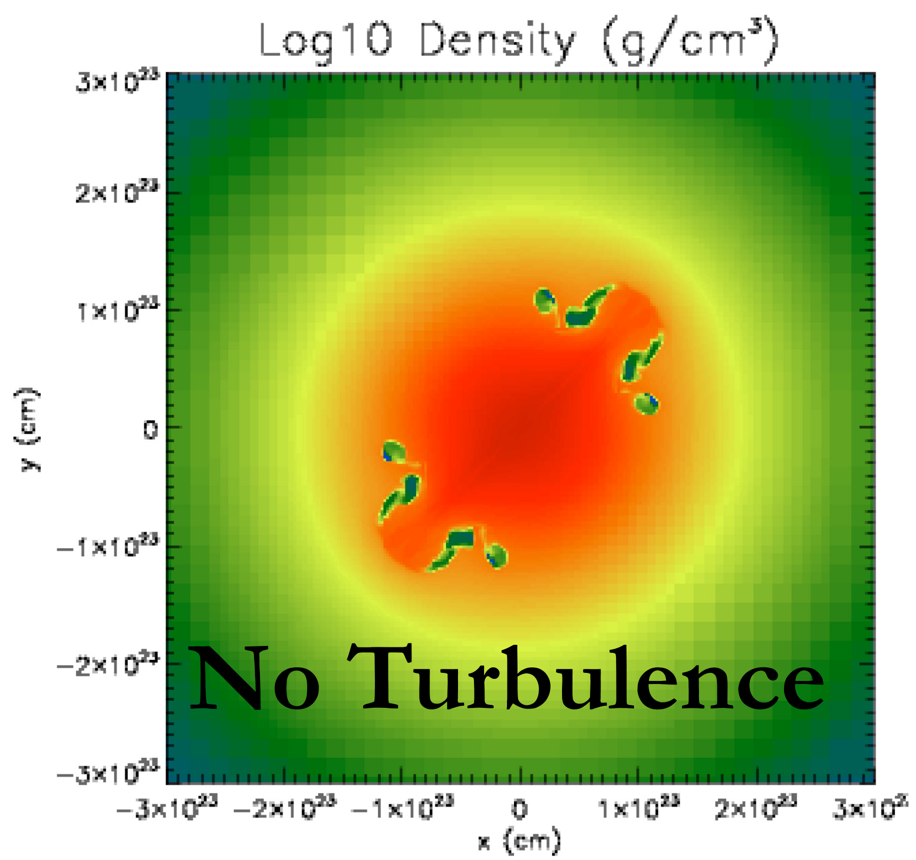

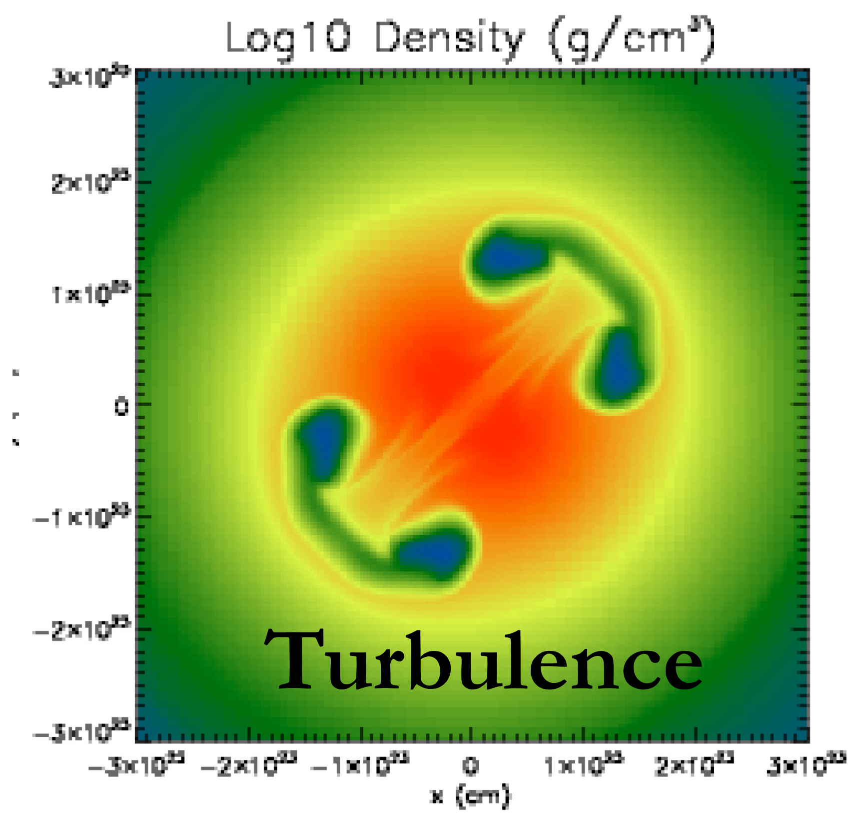

AGN Heating

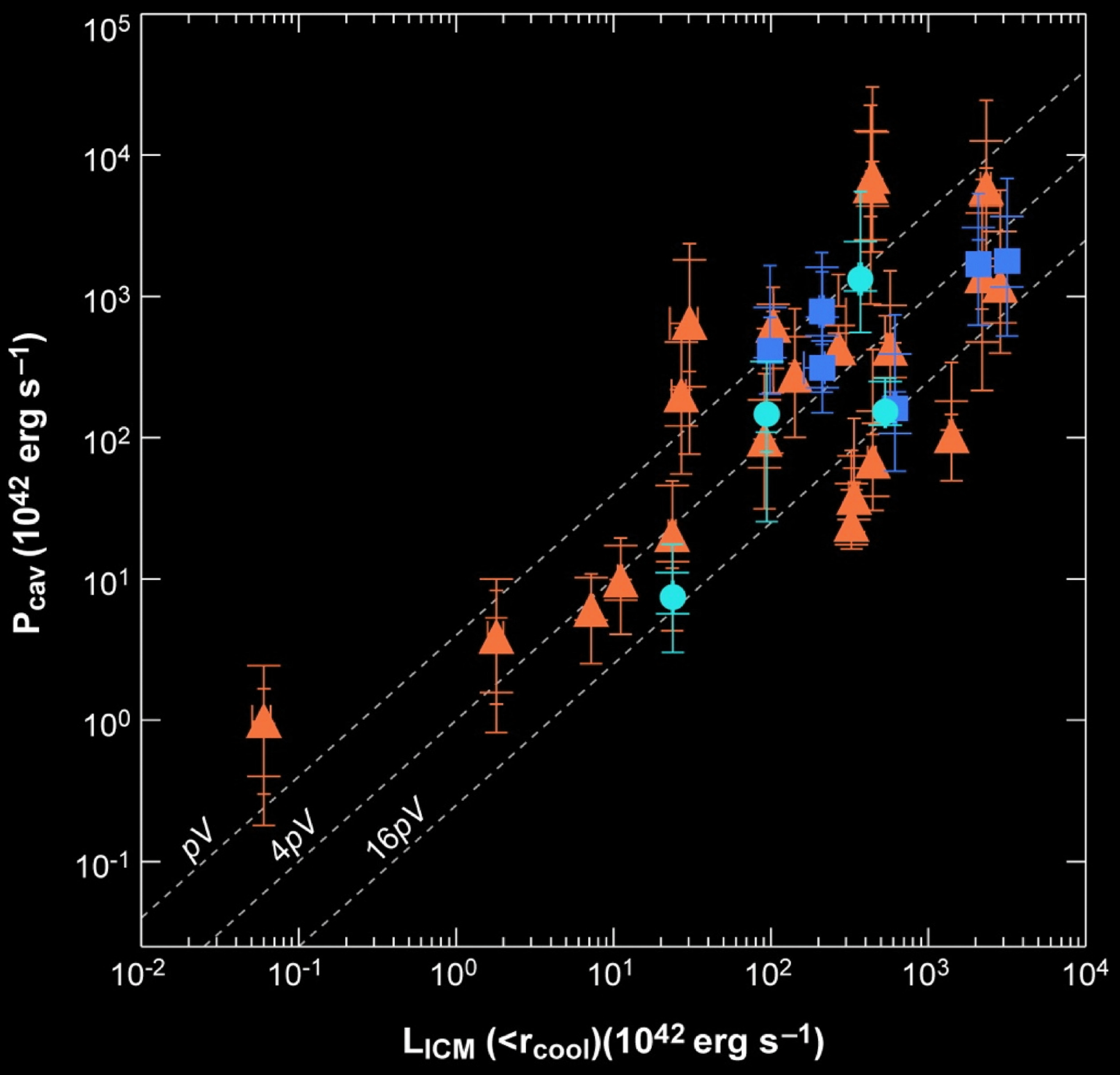

How Coupled?

Rafferty et al. (2006)

Vernaleo & Reynolds (2008)

Low-density channel prevents isotropic heating

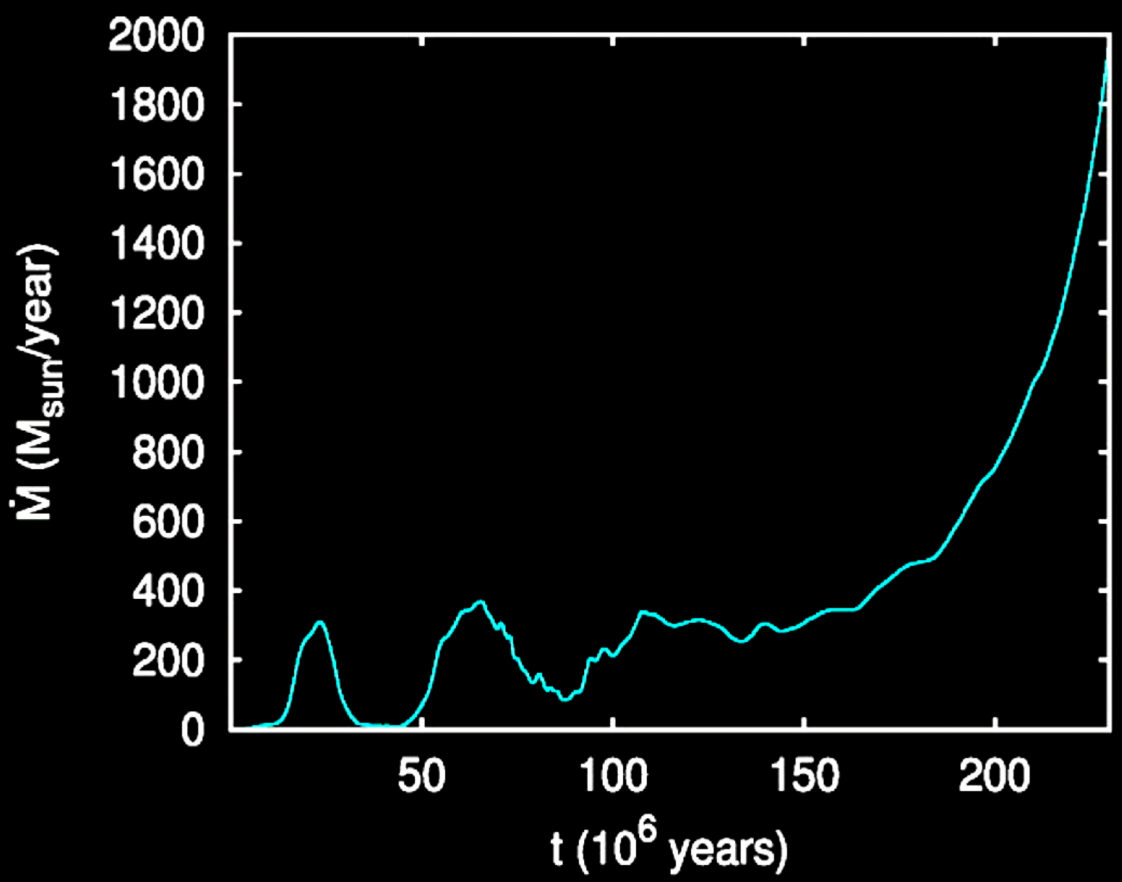

See Also:

Brighenti & Mathews (2006)

Cattaneo & Tessier (2008)

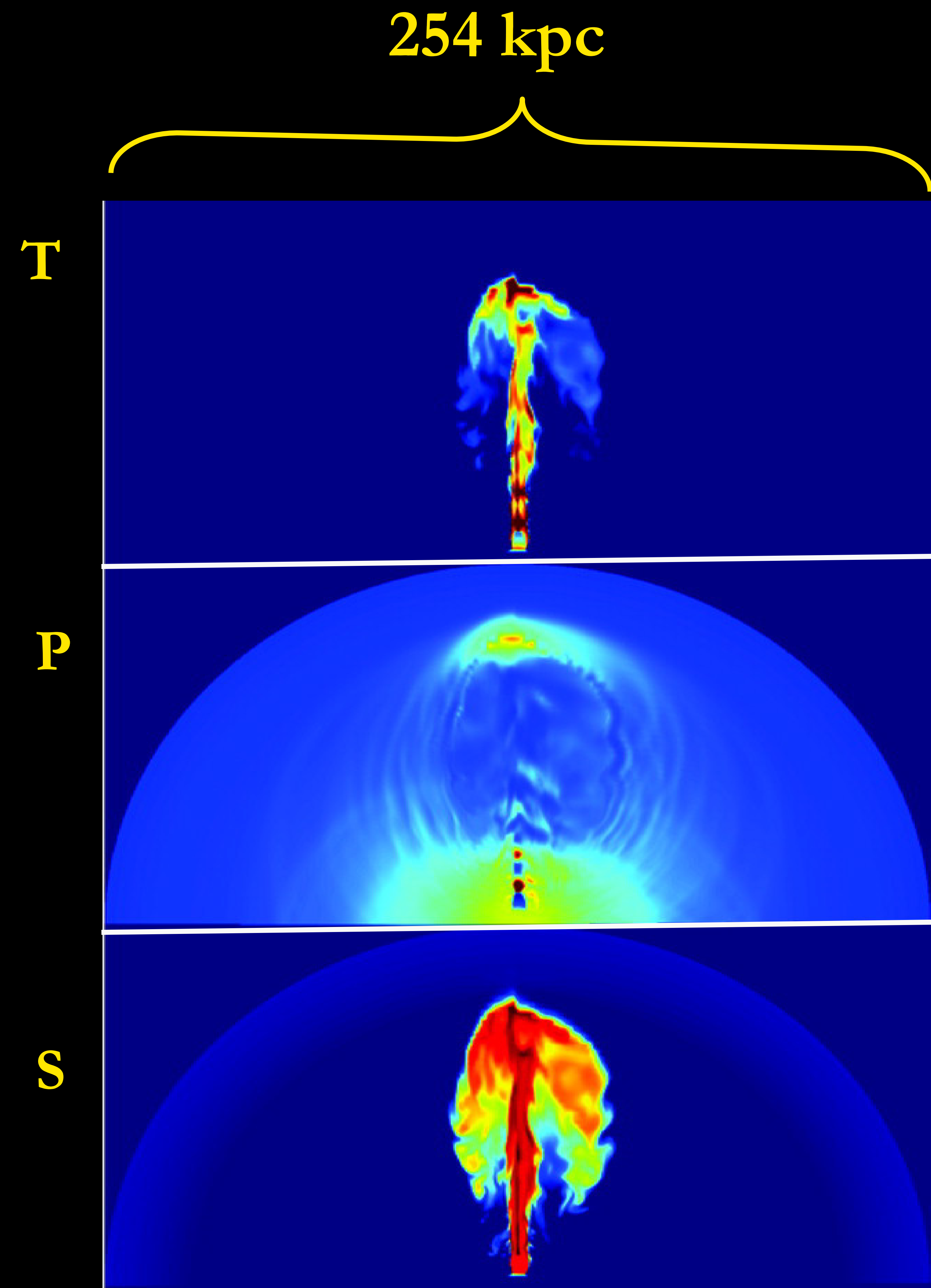

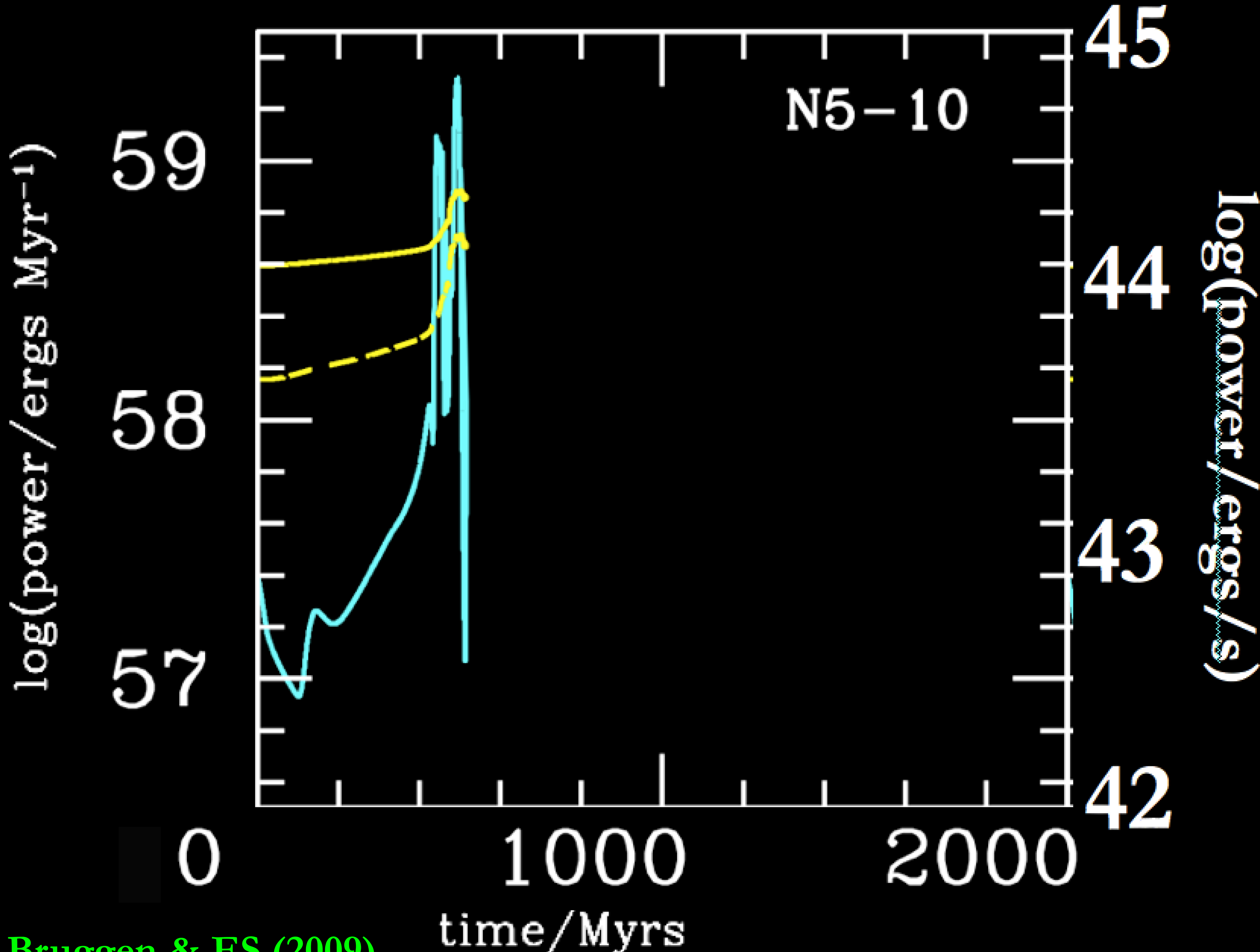

M. Bruggen & ES (2009)

So how do you get the AGN to self-regulate?

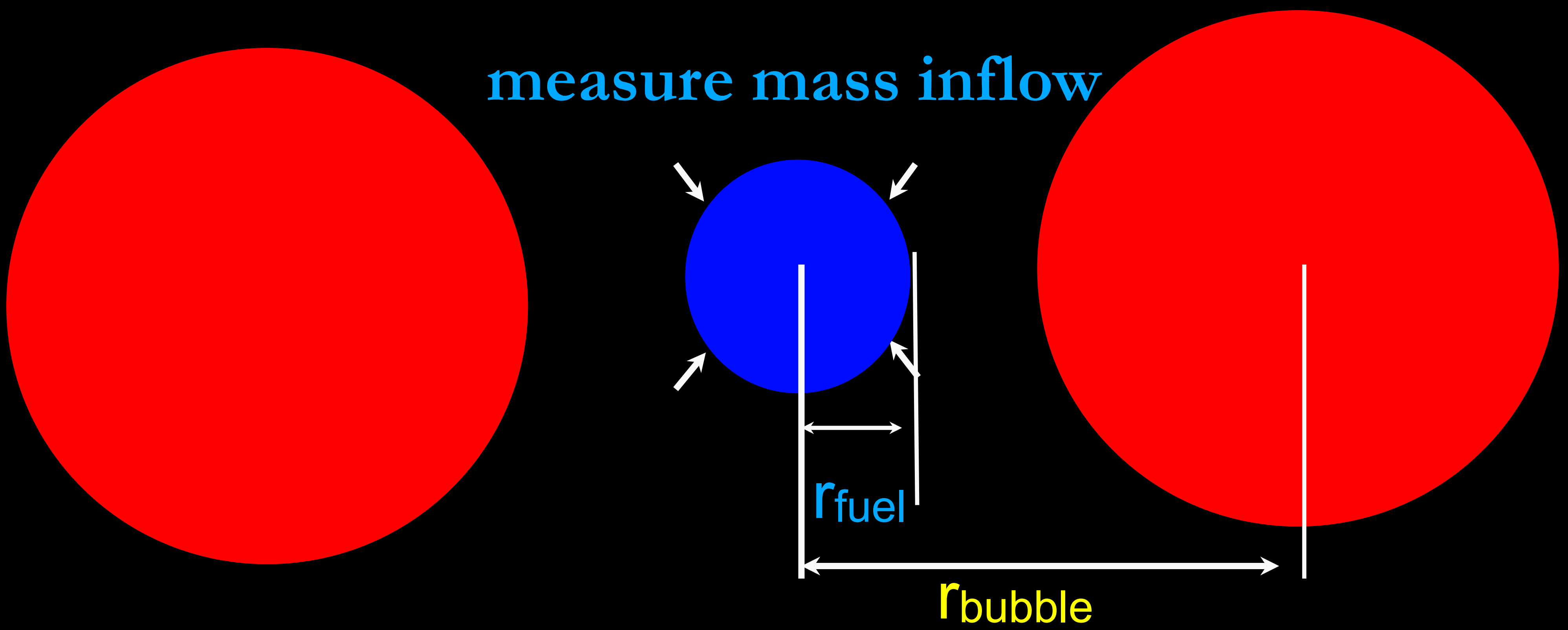

convert a fixed fraction of accreted rest mass energy to bubble energy

M. Bruggen & ES (2009)

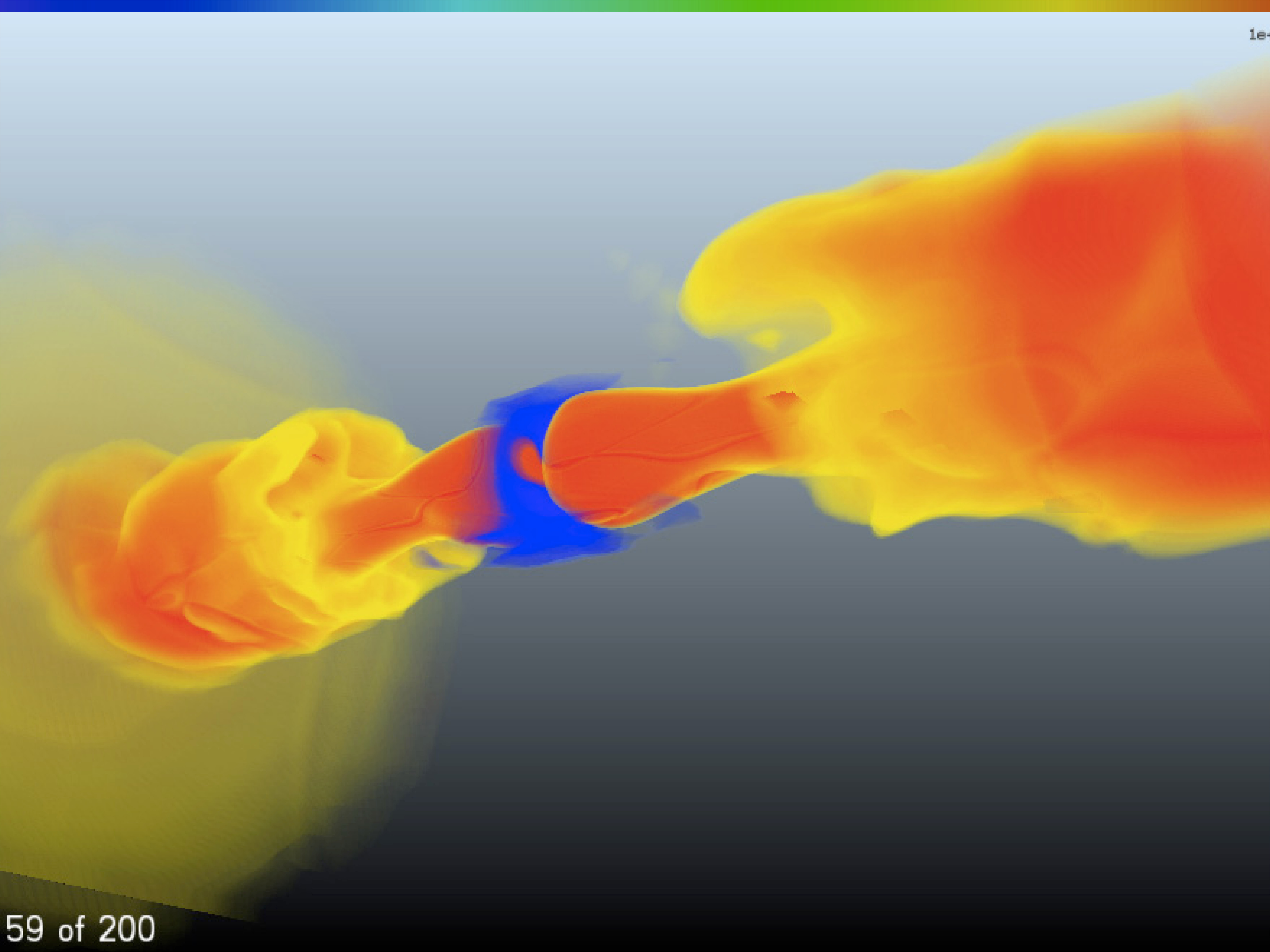
1e-
59 of 200

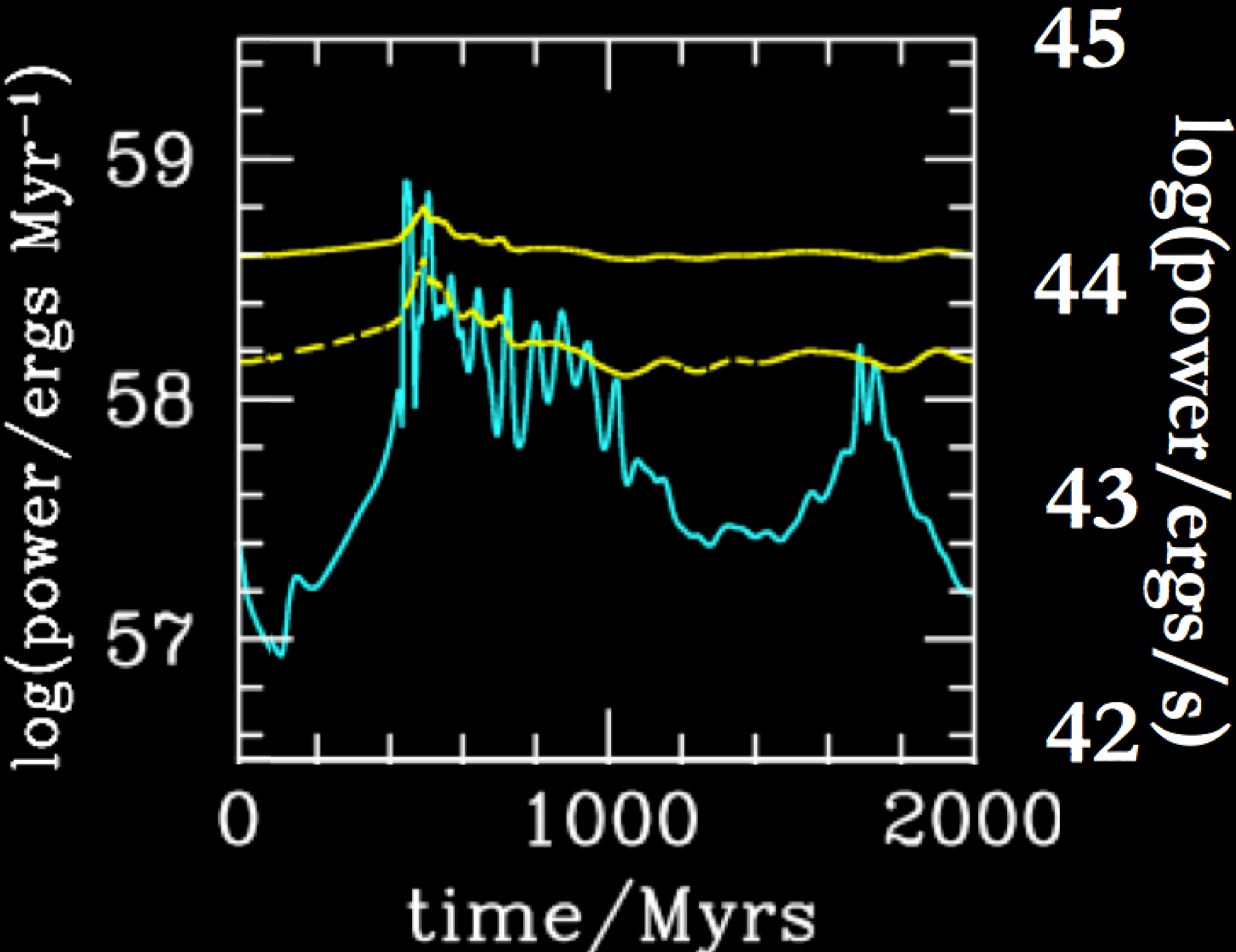

M. Bruggen & ES (2009)

What Sets Duty Cycle?

$$t_{\rm duty} \approx l/v_{\rm turb}$$

$$v_{\rm turb} = gl/c_s \approx c_s \frac{l}{r_0} \quad g = c_s^2 \frac{1}{\rho}\frac{d\rho}{dr} \equiv c_s^2/r_0$$

$$t_{\rm duty} \approx \frac{r_0}{c_s}$$

M. Bruggen & ES (2009)

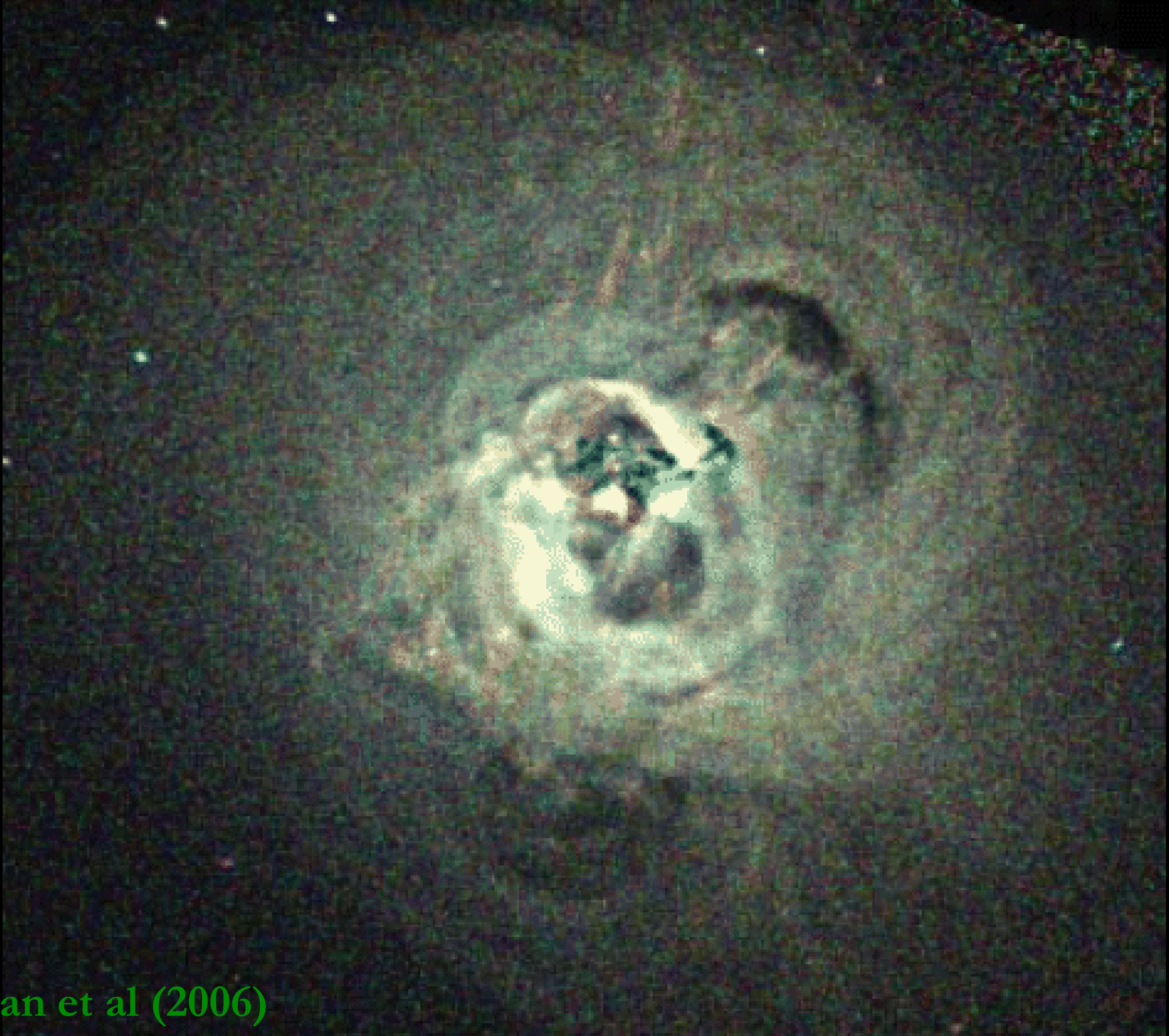
Fabian et al (2006)

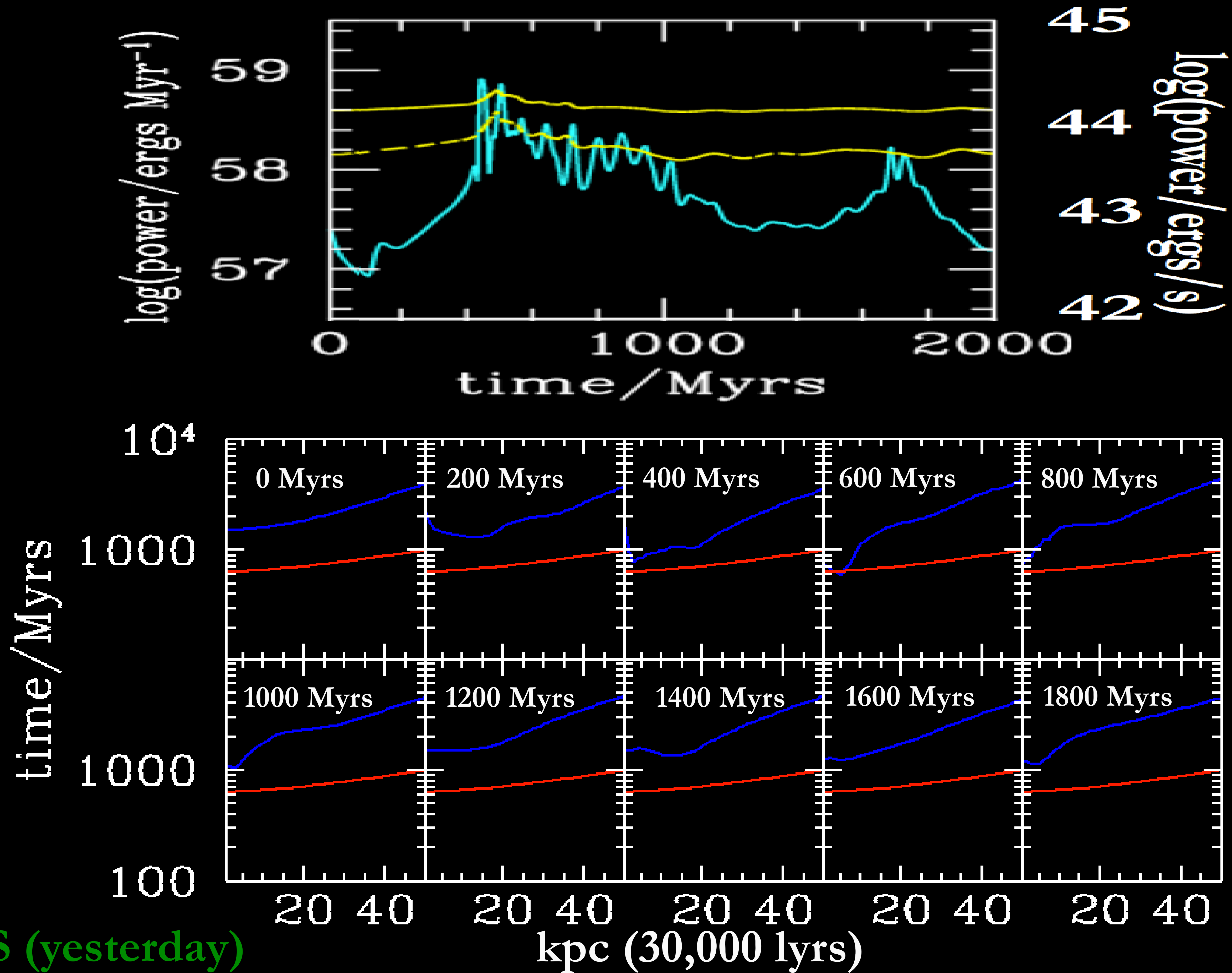

ES (yesterday)

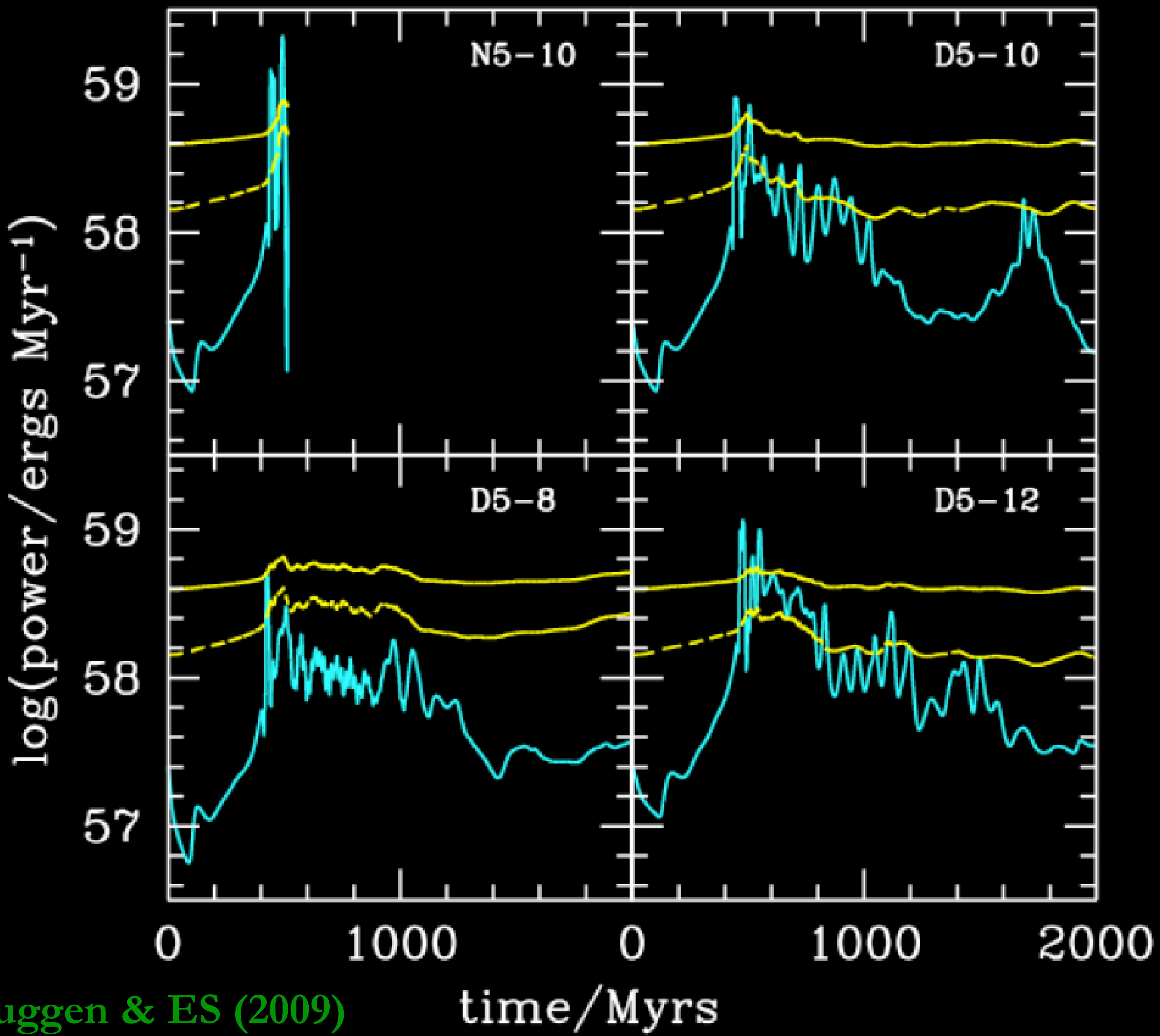

M. Bruggen & ES (2009)

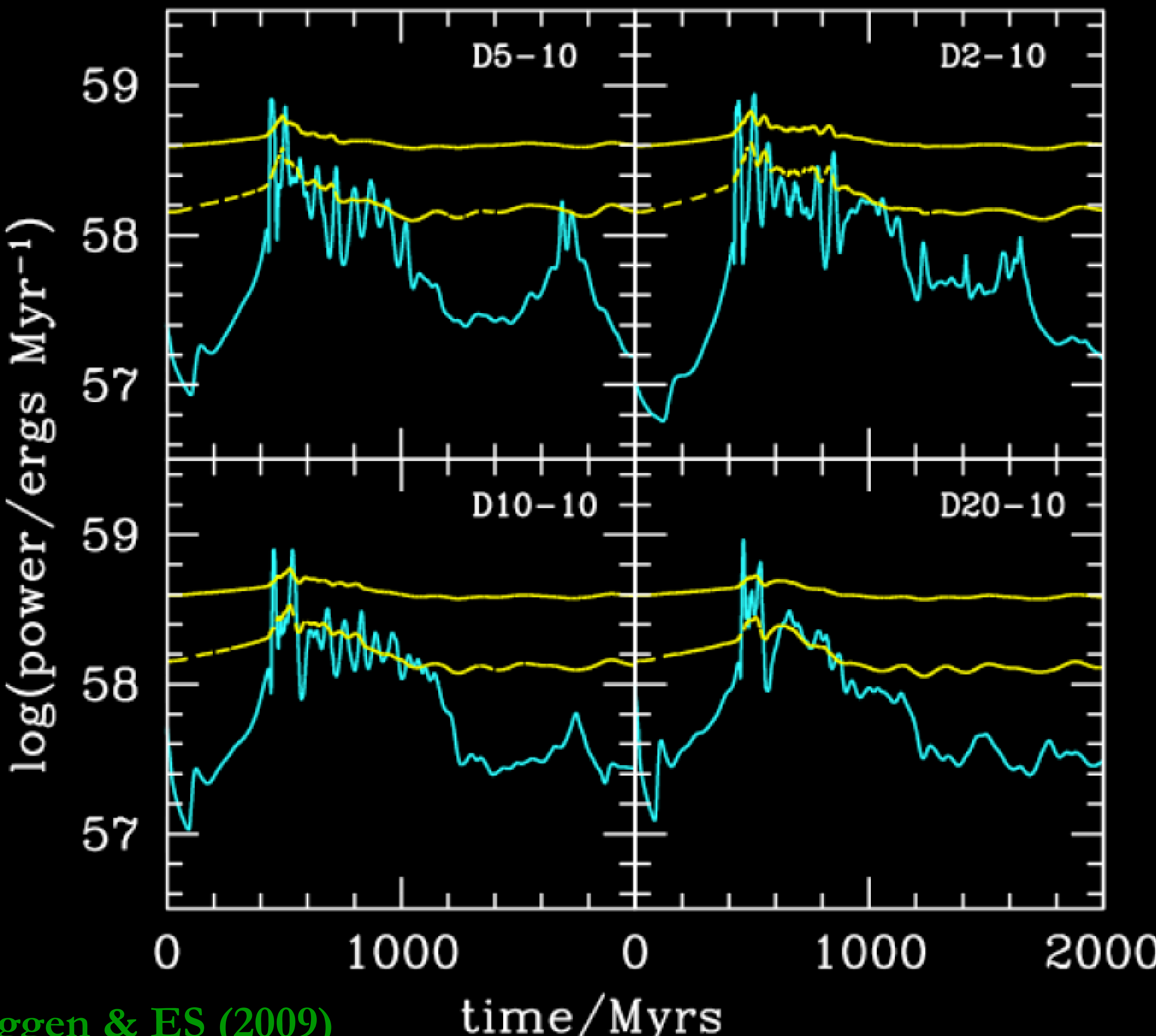

M. Bruggen & ES (2009)

Thanks!

Feedback from black holes and supernovae played a complex but essential part in cosmic structure formation.

To successfully model this we will need:

1.) To develop accurate subgrid turbulence models to span the gap from cosmic scales to the turbulent dissipation scale.

2.) To understand how these models couple with other processes and how they appear observationally.